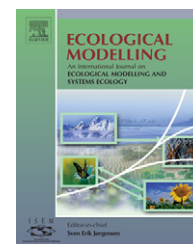


available at [www.sciencedirect.com](http://www.sciencedirect.com)journal homepage: [www.elsevier.com/locate/ecolmodel](http://www.elsevier.com/locate/ecolmodel)

## Assessing functional landscape connectivity for disturbance propagation on regional scales—A cost-surface model approach applied to surface fire spread

Jesus Rodriguez Gonzalez<sup>a,\*</sup>, Gabriel del Barrio<sup>b</sup>, Beatriz Duguay<sup>c</sup>

<sup>a</sup> Instituto de Agricultura Sostenible (IAS), Consejo Superior de Investigaciones Científicas (CSIC), Alameda del Obispo s/n, 14004 Cordoba, Spain

<sup>b</sup> Estacion Experimental de Zonas Aridas (EEZA), Consejo Superior de Investigaciones Científicas (CSIC), General Segura 1, 04001 Almeria, Spain

<sup>c</sup> Centro de Estudios Ambientales del Mediterraneo (CEAM), Charles Darwin 14, Paterna, 46980 Valencia, Spain

### ARTICLE INFO

#### Article history:

Received 29 December 2005

Received in revised form

18 August 2007

Accepted 30 August 2007

#### Keywords:

Cost-distance surface analysis

Landscape model

Functional landscape connectivity

Fire propagation

Fractals

NFFL Fuel models

Scenario modelling

### ABSTRACT

Leaning on concepts from landscape ecology and functional landscape connectivity, we formulated and developed an operational definition of regional connectivity using a cost-surface modelling approach to assess fire connectivity whereby its structural and spatial components are explicitly isolated. Once the model is calibrated, it allows comparing different scenarios of vegetation composition and moisture contents. The use of commonly available input data and an easy to implement method to code resistance to fire propagation for a given landscape facilitates the application of this approach to other areas of interest. Functional landscape connectivity with regard to fire propagation is expressed through cost surfaces that are computed from a fire friction map and a random set of ignition points. The spatial complexity of the cost surfaces is assumed to be proportional to the landscape connectivity, and its fractal properties are used to measure and describe such spatial complexity. The fractal dimension of a cost-surface serves to assess the regional connectivity in terms of the spatial structure of frictions to fire spread, while the mean value of a cost-surface describes the overall resistance to fire propagation across the landscape in a lumped, non-spatial form. The fire friction map is derived using objective and empirically confirmed techniques enabling to account for the major factors of general fire behaviour. Furthermore, an easy to implement and repeatable method is presented to select the optimum size of random sets of ignition points, implicitly fine-tuned to the spatial variation of the input data. The model was tested on running a number of landscape scenarios based on a NFFL fuel model map. An initial series of runs served to select an optimum number of ignition points and to assess the model sensitivity to fuel moisture. Then, a set of three scenarios of vegetation cover change was devised by replacing a fast fuel model by slower fuels, and the existing network of fuelbreaks was also overlaid. The model performed as expected by quantifying the differential resistance to fire spread implicit to such scenarios. As an overall result, our model indicates that reducing the length scale of the landscape texture has a greater effect preventing fire connectivity than creating large, homogeneous patches of fire resistant vegetation.

© 2007 Elsevier B.V. All rights reserved.

\* Corresponding author. Tel.: +34 957 499 258; fax: +34 957 499 252.

E-mail address: [jrodriguez@ias.csic.es](mailto:jrodriguez@ias.csic.es) (J. Rodriguez Gonzalez).

0304-3800/\$ – see front matter © 2007 Elsevier B.V. All rights reserved.

doi:10.1016/j.ecolmodel.2007.08.028

## 1. Introduction

Disturbances (natural or anthropogenic) can be defined as relative discrete events in time that disrupt ecosystems, communities or population structure, and can impact natural resources or the physical environment. This includes both destructive or catastrophic events as well as less notable natural environmental fluctuations. Examples of such natural disturbances that interact with the landscape on regional scales are for example wildland fires, earthquakes, insect outbreaks, severe winds or ice storms. Anthropogenic caused disturbances are, for example, grazing activities or clear-cutting of large forested areas (Gardner et al., 1996; Turner et al., 2001; Peterson, 2002; Chapin et al., 2002). Another way to classify different disturbances is according to their spatial structure and propagation across the landscape into non-contagious and contagious disturbances. Non-contagious disturbances are not altered by changing landscape patterns—a hurricane for example does not change its path because of a road or a fuelbreak in its way. Contagious disturbances on the other hand, for which fire is representative, spread across a landscape dynamically interacting with it. Though once started, the process of fire spreading across a landscape is influenced by a wide range of temporal and spatially variable environmental factors such as wind direction, wind strength, rainfall or fuel moisture among others. This process is also, and not less importantly, influenced by landscape specific features like terrain topography, fuel availability, fuel type and fuel spatial distribution (Chandler et al., 1983; Pyne, 1984; Kerby et al., 2007). An advancing fire front cannot propagate if it encounters a sufficiently large fuel-less area. In short, fire needs the landscape to be ‘connected’ by means of continuous and flammable fuel patches to successfully propagate through it (Miller and Urban, 2000; Peterson, 2002).

Landscape ecology has emerged by combining the spatial approach of regional geography and the functional approach of ecology, and it is focused on the influence of the landscape structure on ecological processes (Turner et al., 1989; Turner et al., 2001). Merriam (1984) was first introducing the term of landscape connectivity, defining it as the interaction between a species features and the landscape structure on the movement of the species populations across a certain territory. Thus, any propagation process does not only depend on the species alone, but also on the landscape and its structure influencing the species behaviour (Tischendorf and Fahrig, 2000a). Two approaches towards connectivity are generally distinguished: structural and functional (Forman, 1995). Structural connectivity is concerned with the spatial distribution and contiguity of habitats across a landscape, often excluding attributes of the species in question. It is measured and analyzed using a wide range of parameters developed to describe the topological structure of landscape patches (Hargis et al., 1998; Gustafson, 1998). The functional approach considers connectivity as a landscape attribute which depends also on the properties of a given species. According to Taylor et al. (1993) landscape connectivity “... is the degree to which the landscape facilitates or impedes movement among resource patches”. Thus the same landscape is experienced differently by diverse organisms. Species perceive and interact with the

same landscape at different spatial scales and are influenced by different landscape features according to their overall environmental niche (del Barrio et al., 2000; Goodwin, 2003). This idea can be conveniently generalized to the movement or propagation across a territory of a dynamic process that depends on landscape properties. This work aims at applying the concept of functional connectivity to the process of fire spread.

The complex interactions between crown or surface fire disturbances and landscape patterns have been studied using a wide range of different models (Green, 1983; Gardner et al., 1987; Turner et al., 1989; Turner and Romme, 1994; Pausas, 2003). In recent years, the models applied have moved to more complex and advanced landscape dynamic models like the ZELIG forest gap model (Miller and Urban, 1999a,b, 2000), the EMBYR model (Hargrove et al., 2000), the LANDIS model (Mladenoff and He, 1999; He and Mladenoff, 1999; Gustafson et al., 2000) or models based on cell automata (Karafyllidis and Thanailakis, 1997; Encinas et al., 2007). Those models simulate concrete fire events under dynamic conditions including weather factors. They are possibly the best approach for real-time simulation of evolving fires, and are to be used whenever the position of an advancing fire front should be forecasted (Coleman and Sullivan, 1996; Fujioka, 2002). However, they pose an intrinsic difficulty to assess the contribution of the landscape structure to the fire spread, as dynamic factors must be fixed by holding them constant (Duncan and Schmalzer, 2004). For that reason, their use in landscape planning and management is often associated to typical weather and starting ignition conditions (e.g. Miller and Yool, 2002; Mistry and Berardi, 2005), hence representativeness is somewhat limited. We propose here a new approach to model and assess functional landscape connectivity for surface fire propagation using a spatially explicit landscape model based on cost surfaces.

Though the potential and possibilities of cost-distance surfaces were early discovered (Warntz, 1965), only in the last few years has this methodology gained more attention especially in ecological and population modelling (for examples see del Barrio et al., 2000; Michels et al., 2001; Adriaensen et al., 2003; Chardon et al., 2003; Verbeylen et al., 2003; del Barrio et al., 2006; Röder et al., 2007). This is most likely due to the fact that suitable cost-distance algorithms are now included into the available standard GIS software packages (Adriaensen et al., 2003). The cost-distance modelling approach requires two raster layers. In this work, the ‘friction surface’ or resistance layer assigns a resistance to fire propagation to each single landscape cell. The source layer indicates the spatial location of the initial feature points, the ignition points in this case. Based on the friction surface, a cost-distance algorithm calculates the minimum cumulative resistance, or least-costs, for a fire to propagate to every landscape cell from its nearest ignition point. In the resulting ‘cumulative least-cost distance surface’ (‘cost-surface’ for short) each value represents the difficulty of a spreading fire to reach any location along the path which offers the least resistance in terms of cumulative friction or costs. The use of paths of minimum travel time between fire nodes was already suggested by Finney (2002), and it is greatly simplified by the least-cost method proposed in our model.

The resulting three-dimensional cost-distance surface conveys the spatial structure of functional connectivity for fire propagation on a regional level. While this has mapping value on its own, the comparison among different scenarios would be greatly facilitated if a numerical indicator were used. To quantitatively measure functional connectivity, Tischendorf and Fahrig (2000a,b) recommend, that whatever measurement of connectivity is used, it should reflect the movement or process in question among resource patches over the entire landscape, and it should quantify properly the exact definition of functional landscape connectivity. We have used the fractal dimension to assess the geometric complexity of the cost-distance surface across the whole landscape through one single, intuitive numerical parameter (Leduc et al., 1994; del Barrio et al., 2000). To the authors' best knowledge, this approach has so far not been used in conjunction with fire propagation and functional landscape connectivity. It contributes through specific objectives to the range of available models in fire ecology. But from a broader perspective, this work aims also at formalizing some basic elements of ecological connectivity. This is done through two new contributions. First, the use of explicit functions controlling the affinity of the movement for each landscape location, rather than using empirical relationships as it is done normally when working with biological species. And second, the use of a suite of parameters of spatial structure to compare surfaces generated from different configurations of a driving factor.

The specific objectives of this work were:

- (1) to develop an objective method to code the friction surface of fire prone landscapes, such that the fundamental factors governing fire propagation are accounted for and can serve as a true representation of functional connectivity;
- (2) to test the use of fractal indices to quantify functional connectivity for fire propagation on a regional scale;
- (3) to test the ability of our model to detect and quantify the influence of changing vegetation (fuel) cover using different scenarios with and without fuelbreaks.

In general these objectives are concerned with setting up a modelling framework to assess landscape connectivity for fire propagation under different scenarios of fuel distribution. A study region located in the Western Mediterranean has been used to parameterize the model through the adaptation of available data, and model runs and simulation scenarios have been designed to test the model performance. In this context, the creation of a realistic model assembly and testing has received priority over making a realistic representation of the fuel composition and fire dynamics in a case study region.

## 2. Methods and techniques

### 2.1. Study region

The Ayora Region is located in Eastern Spain within the Autonomous Community of Valencia. It covers an area of approximately 3300 km<sup>2</sup>. In general terms, the region is characterized by a diversified and rugged topography. Altitude ranges from 20 m.a.s.l. to nearly 1200 m.a.s.l. The central part

consists of an undulated area with an average elevation of about 600–700 m.a.s.l., which is interrupted by steep slopes and the valleys of the rivers Rio Grande and Escalona draining the region in easterly direction into the Jucar river and to the coastal plains. West of this central area, running straight from south to north, lies the Ayora-Cofrentes valley.

The climate is typically Mediterranean, with hot and dry summer months and a mild winter. The average annual temperature ranges from 13 to 18 °C. Mean annual precipitation varies between 350 and 750 mm, showing a bimodal distribution with main maximum rainfalls in late autumn and early winter months, and a secondary maximum in April or May. Though all months receive rainfalls, the dry season between July and August–September limits the vegetative period to 8–11 months. Potential evapotranspiration reaches its yearly maximum during summer, causing a negative regional water balance and extremely low moisture content of the vegetation cover, and a very high fire-proneness in the region.

Rangelands account for 67% of the total land use and are largely dominated by dense shrublands and, to a lesser degree, by pine forests. These shrublands consist mainly of *Quercus coccifera* oaks with *Ulex parviflorus* and/or *Rosmarinus officinalis*. The pine forests are dominated by *Pinus halepensis* and more rarely *Pinus pinaster*. Today, the typical Mediterranean woodland formations of *Quercus ilex*, *P. pinaster* and *Pinus halepensis* are only found on small remote and isolated areas. Agriculture is concentrated on the more suitable areas of the eastern plains and along the Ayora-Cofrentes valley. The mountainous areas, once under traditional, labour intensive cultivation were left behind. This has led, in particular at the end of the 1960s and the beginning of the 1970s, to high fuel concentrations on once cultivated areas enhancing the natural fire-prone environmental conditions of the region.

### 2.2. Datasets used

#### 2.2.1. Digital elevation model and slope layer

The digital elevation model (DEM) is required to derive the slope values for calculating the potential maximum rate of spread, which serves as one of the main parameter in this approach to code the friction surfaces. The raster DEM for this work was derived from 10 m contour lines from 1:25,000 topographic maps of the Spanish *Servicio Geográfico del Ejército*, and its original resolution of 25 m was resampled to 30 m using a bilinear interpolation. The slope layer was extracted using the algorithm implemented in the IDRISI32 GIS software (Eastman, 2001).

#### 2.2.2. Fuel model layer

Based on the Spanish National Forest Map from 1993 (MAPA, 1993) the Ayora region was reclassified using the photographic identification key of the Spanish Forest Administration (MAPA-ICONA, 1990), which assigns to each of the main vegetation structural types of eastern Spain one of the 13 National Forest Fire Laboratory (NFFL) standard fuel models (Albini, 1976; Anderson, 1982). Throughout this work we used an early version of the fuel model layer that was made available to us. Table 1 shows the percentage of each of the fuel models found in the Ayora region, and their spatial distribution across the Ayora region is presented in Fig. 1. As can be seen, the largest

**Table 1 – Fuel models in the Ayora study region**

| Fuel model | Typical fuel complex          | Percentage of total |                       |
|------------|-------------------------------|---------------------|-----------------------|
|            |                               | Study region (%)    | Fuel covered area (%) |
| 1          | Short grass                   | 2.9                 | 5.0                   |
| 2          | Timber (grass and understory) | 4.6                 | 7.8                   |
| 3          | Tall grass                    | 10.3                | 17.6                  |
| 4          | Chaparral                     | 23.1                | 39.4                  |
| 5          | Brush                         | 6.4                 | 10.8                  |
| 6          | Dormant brush, hardwood slash | 0.1                 | 0.2                   |
| 8          | Closed timber litter          | 11.3                | 19.2                  |

Percentages refer to total area of the study region (left) and to total fuel covered area (right). Note that only approximately 60% of the total area of the Ayora study region is covered by fuels.

part of the region belongs to the category of fast fuels through which fire can easily spread at high propagation rates.

2.2.3. Fuelbreak layer

Fuelbreaks in Ayora are ranked in three orders of importance, with a width ranging from 1 to 70 m. The fuelbreak layer was rasterized from the version provided in vector format. Because the cell resolution is larger than the width of the fuelbreaks in many cases, only segments aligned with the northing and easting directions could be represented by a closed chain of cells after rasterization. Diagonal segments are approximated by a stepped line of cells, thus allowing the cost algorithm to cross the fuelbreaks through the diagonal cracks without reflecting the higher costs that should be associated with the crossing of them. Rothley (2005) and Theobald (2005) provide

an overview of the problems associated with cracks in friction or resistance layers for cost-distance analysis. To overcome this problem, we added a buffer of one cell to the rasterized fuelbreak lines. Since the fuelbreaks are now three cells wide, accuracy in location has been sacrificed in order to increase the explaining power of the landscape model (Schneider and Robbins, 1994). The fuelbreak network was incorporated to this model as relative barriers, i.e. barriers which are very difficult to cross, but do not impede movement across them *a priori* by declaring them absolute barriers for fire propagation.

2.3. Procedure for estimating regional connectivity

The whole procedure we propose for estimating functional connectivity is visualized in Fig. 2 and can be broken down

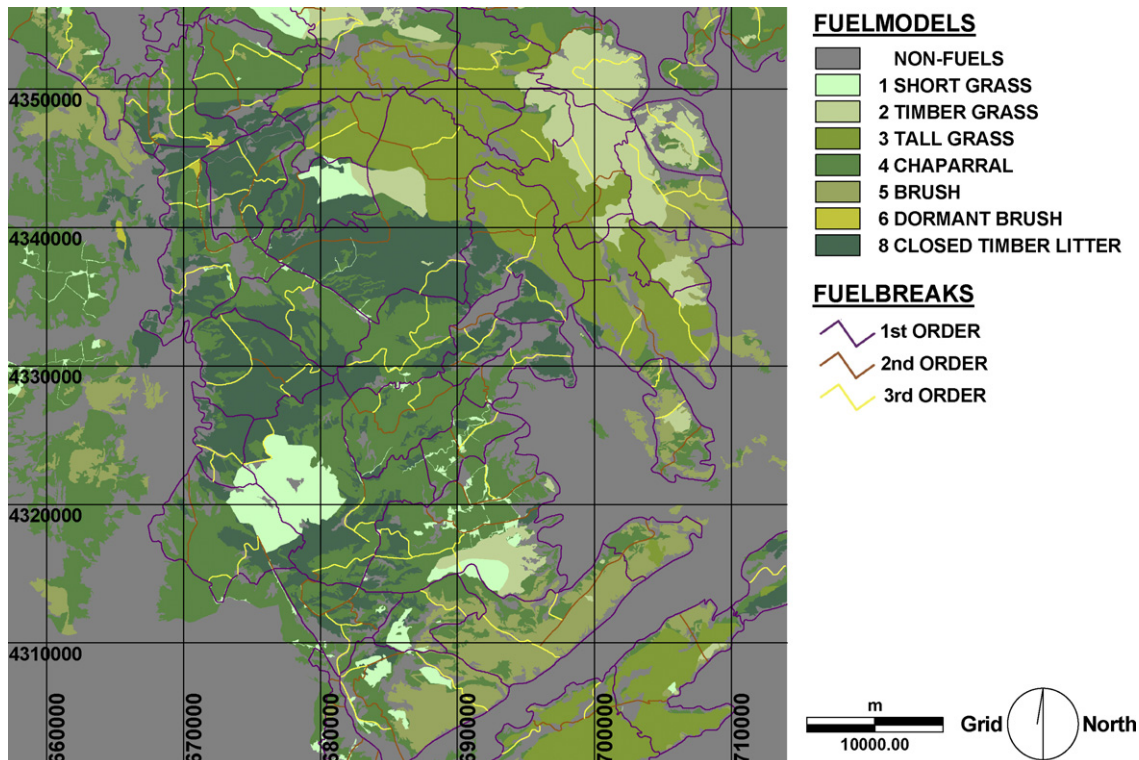


**Fig. 1 – Overview of the Ayora study region: spatial distribution of fuels and fuelbreak network. The grid coordinates are in UTM.**

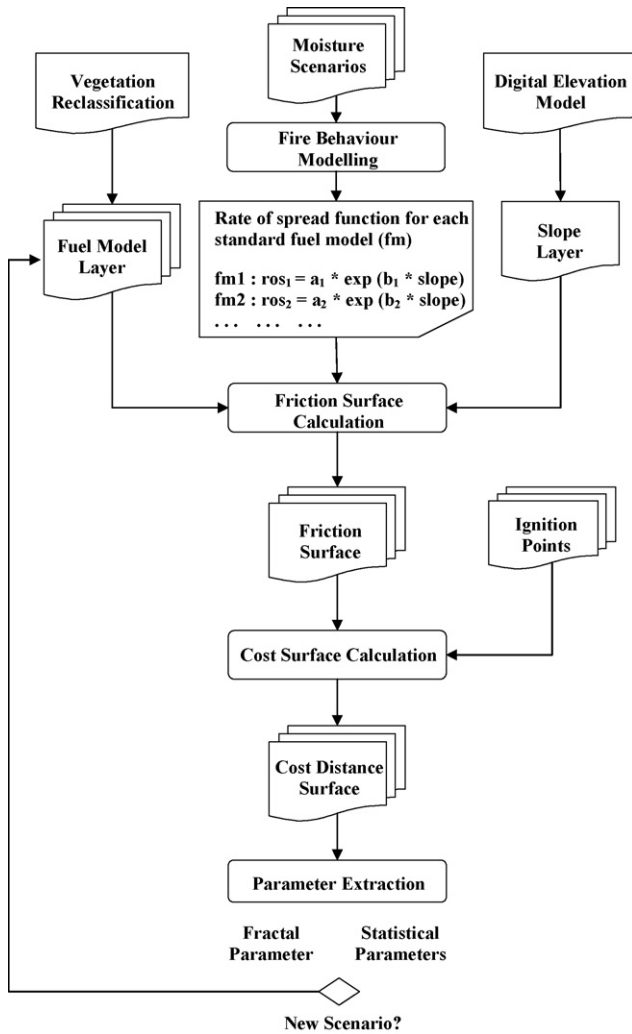


**Fig. 2 – Overview of the essential steps of the presented procedure.**

into its essential parts as follows: (i) the calculation of the cost surface as a spatially distributed estimate of the landscape connectivity for fire propagation; (ii) the extraction of fractal properties as an indicator of the spatial structure of such a surface that can be used to compare different scenarios; and (iii) the final analysis and interpretation of the results.

**2.3.1. Cost-distance surface modelling**

As already mentioned, two raster layers and a cost-algorithm are required to model a cost surface. The friction layer represents a numerical estimate of the ‘true’ resistance encountered by a spreading fire in any given landscape cell, and the feature layer contains the spatial location of the ignition points to initialize fire spread and cost-calculation. The CostGrow algorithm implemented in the GIS package IDRISI is used in this study. It can handle large and complex friction surfaces including relative and absolute barriers. Fire spread is possible from any given cell into all eight adjacent ones: the four cardinal directions and the diagonals. A correction factor of  $\sqrt{2}$  is applied for diagonal movements accounting for the longer cost-distance. If more than one feature or ignition

point is present, the algorithm also identifies the nearest feature point corresponding to each cell in terms of cost-distance. This, as well as a greater complexity of the underlying friction surface, is achieved at the expense of a rapidly increasing number of passes or scans with the resulting increase in processing time (Eastman, 1989; Eastman, 2001).

2.3.1.1. From factors influencing fire propagation to friction values. Coding of the friction surface is essential in this modelling framework. The effect of using wrong or arbitrary friction values that do not reflect the relative differences of fire resistance of different landscape features is that spatial contrasts of the resulting cost surfaces are changed or blurred. The friction surface, to be both reliable and credible, should be coded preferentially based on empirical data rather than on expert judgement or on a set of arbitrary values (Tischendorf and Fahrig, 2000b; Chardon et al., 2003). The most important factors influencing fire spread are usually resumed under the known term of fire-triangle: fuels – weather – topography (Chandler et al., 1983). It is therefore essential that they are included into the friction layer. With this arises a general problem of cost-surface modelling that has to be addressed. Any movement or propagation process is usually influenced by several factors, rather than a single one. Whenever it is necessary to consider more than one input factor and to include them into the friction layer, weighting coefficients are required to combine all desired factors into one single friction layer. These weighting coefficient must represent the relative importance of each of the factors. To overcome this problem Verbeylen et al. (2003) for example tested several resistance sets, and Röder et al. (2007) relied on expert judgement. To avoid an extensive test procedure to approach experimentally the correct weighting coefficients, or testing a high number of different friction sets, we propose to resort to established fire behaviour prediction methodology. The Rothermel model (Rothermel, 1972) was used here to derive an objective and reliable estimate of the resistance of each single landscape cell towards fire propagation.

The semi-physical Rothermel fire spread model is based on an energy balance and the law of conservation of energy (Frandsen, 1971) and predicts the quasi-steady rate of spread at the head of an advancing surface fire front independently from its ignition point under no-slope and no-wind conditions. After the influence of wind and slope are accounted for by correction coefficients, the rate of spread ROS (m/min) is given by

$$ROS = \frac{I_R \mu}{\rho_b \epsilon Q_{ig}} (1 + \phi_w + \phi_s) \tag{1}$$

where  $I_R$  is the reaction intensity (m/min),  $\mu$  the propagation flux ratio (kJ/min m<sup>2</sup>),  $\rho_b$  the oven-dry bulk density (kg/kg<sup>3</sup>),  $\epsilon$  the effective heating number,  $Q_{ig}$  the heat of pre-ignition (kJ/kg),  $\phi_w$  the wind coefficient and  $\phi_s$  is the slope coefficient.

Under the assumption of no-wind conditions, the potential maximum rate of spread  $ROS_{max}$  is always reached in the direction of maximum slope, and therefore depends only on fuel type, fuel moisture content and slope of each landscape cell. Dividing the cell size (in this case defined by the 30m reso-

**Table 2 – The NFFL standard fuel models used in fire behaviour modelling (Albini (1976), cited in Anderson (1982) and Velez (2000a); modified)**

| Fuel model                 | Typical fuel complex           | Fuel loading (t/ha) |      |       |      | Total | Fuel bed depth (m) | Moisture of extinction of dead fuels (%) |
|----------------------------|--------------------------------|---------------------|------|-------|------|-------|--------------------|--|
|                            |                                | 1 h                 | 10 h | 100 h | Live |       |                    |  |
| Grass and grass-dominated  |                                |                     |      |       |      |       |                    |  |
| 1                          | Short grass                    | 1.6                 | –    | –     | –    | 1.6   | 0.3                | 12                                       |
| 2                          | Timber (grass and understory)  | 4.5                 | 2.2  | 1.1   | 1.1  | 8.9   | 0.3                | 15                                       |
| 3                          | Tall grass                     | 6.7                 | –    | –     | –    | 6.7   | 0.8                | 25                                       |
| Chaparral and shrub fields |                                |                     |      |       |      |       |                    |  |
| 4                          | Chaparral                      | 11.2                | 9    | 4.5   | 11.2 | 35.9  | 2.0                | 20                                       |
| 5                          | Brush                          | 2.2                 | 1.1  | –     | 4.5  | 7.8   | 0.6                | 20                                       |
| 6                          | Dormant brush, hardwood slash  | 3.4                 | 5.6  | 4.5   | –    | 13.5  | 0.8                | 25                                       |
| 7                          | Southern rough                 | 6.5                 | 4.2  | 3.4   | 0.83 | 20.9  | 0.8                | 40                                       |
| Timber litter              |                                |                     |      |       |      |       |                    |  |
| 8                          | Closed timber litter           | 3.4                 | 2.2  | 5.6   | –    | 11.2  | 0.1                | 30                                       |
| 9                          | Hardwood litter                | 6.5                 | 0.9  | 0.3   | –    | 7.7   | 0.1                | 25                                       |
| 10                         | Timber (litter and understory) | 6.7                 | 4.5  | 11.2  | 4.5  | 26.9  | 0.3                | 25                                       |
| Slash                      |                                |                     |      |       |      |       |                    |  |
| 11                         | Light logging slash            | 3.4                 | 10.1 | 12.3  | –    | 25.8  | 0.3                | 15                                       |
| 12                         | Medium logging slash           | 9.0                 | 31.4 | 37    | –    | 77.4  | 0.8                | 20                                       |
| 13                         | Heavy logging slash            | 15.7                | 51.6 | 62.8  | –    | 120.1 | 1.0                | 25                                       |

lution) by the  $ROS_{max}$  we obtain an estimate of the potential transit time  $T_{pot}$  that a fire front advancing at the potential maximum rate of spread  $ROS_{max}$  needs to spread through it and is given by the following simple equation

$$T_{pot} = \frac{\text{size}_{\text{pixel}}}{ROS_{max}} \quad (2)$$

where  $\text{size}_{\text{pixel}}$  is the cell size or pixel resolution and  $ROS_{max}$  is the potential maximum rate of spread under no-wind conditions.

The Rothermel model fire spread model is widely used in fire ecology and modelling and is included into the fire behaviour prediction system *BEHAVE* (Burgan and Rothermel, 1984; Andrews, 1986; Andrews and Chase, 1989; Andrews et al., 2003), as well as the fire area simulator *FARSITE* (Finney, 1998). Based on laboratory fire experiments, several empirical equations were formulated to substitute the equation terms as functions of measurable values for fuel loading, fuel depth, fuel particle surface-to-volume ratio, particle density, moisture content, mineral content, wind speed, slope and moisture of extinction (Rothermel, 1972; Chandler et al., 1983). The concept of fuel models arose as a convenient method to represent the main and most likely vegetation structural types found in the field, through a stylized set of models according to the main vector of fire spread and expressed by numerical values for the input parameters above mentioned required by the Rothermel model (see Table 2). The fuel moisture scenarios, a set of five moisture content values for different vegetation parts also called timelag classes (Table 3), are necessary to solve the Rothermel equation for fire spread. The three moisture scenarios (low, medium and high) used here for the sensitivity analysis are based on empirical data and represent average mean values at different fire-hazard levels found under typical environmental conditions, and are rec-

ommended when no site-specific data is available (Burgan and Rothermel, 1984). In this sense, they can also be seen as season specific mean values representing changes imposed by seasonal weather changes in fire-hazard levels. The moisture scenario values used in this work for the scenario testing exercise are region-specific values of the Ayora region and stand for extreme fire-risk conditions. This set of values became available at a later stage of the work and for that reason could not be used for the initial sensitivity analysis.

Since *BEHAVE* does not handle raster layers and provides results in tabular form only, we used it to calculate the  $ROS_{max}$  for each of the NFFL fuel models present in the fuel layer map assuming no-wind conditions at slope-steps of 5% and for all of the moisture scenario sets we finally used. A logarithmic regression was fitted to each fuel model and moisture scenario, such that  $ROS_{max}$  is expressed as a function of the slope of each landscape cell for each fuel model and each moisture scenario. This simple procedure allows us to conveniently apply Eq. (2) within the GIS environment to calculate

**Table 3 – Fuel moisture contents for low, medium and high moisture scenario used in the sensitivity analysis**

| Fuel-load class          | Moisture scenario |       |        |      |
|--------------------------|-------------------|-------|--------|------|
|                          | Low               | Ayora | Medium | High |
| Dead 1-h moisture        | 3                 | 4     | 6      | 12   |
| Dead 10-h moisture       | 4                 | 6     | 7      | 13   |
| Dead 100-h moisture      | 5                 | 8     | 8      | 14   |
| Live herbaceous moisture | 70                | 100   | 120    | 170  |
| Live woody moisture      | 70                | 100   | 120    | 170  |

The Ayora moisture scenario is later used for the scenario testing procedure. The values are in (%) of dry weight of fuels.

the underlying friction surface as needed for each of the simulation runs.

The 13 NFFL standard fuel models we use have been established as generalized expected mean values of vegetation groups found throughout the United States with similar fire behaviour (Anderson, 1982), and we are aware of the limitations associated with them when applied to vegetation in Southern Europe. In particular, when the aim is an accurate simulation of fire behaviour and fire spread in time and space in a specific region, it becomes necessary to develop and parameterize custom fuel models. Nonetheless, the 13 NFFL standard fuel models, as well as custom fuel models are commonly used in conjunction with either BEHAVE or FARSITE to investigate and simulate the effects of fuel and management activities in European Mediterranean regions (Velez, 2000a; Fernandes and Botelho, 2004; Duguay et al., 2007). Procedures and general concepts for establishing custom fuel models can be found in Burgan and Rothermel (1984) and Burgan (1987) and for the specific case of Spain in MAPA-ICONA (1990). Part of this problem is possibly mitigated by the recent introduction of an extensive set of additional fuel models (Scott and Burgan, 2005) which, though they might as well require a region specific parameterization, appear to be far more suitable for the predominant vegetation patterns and types found throughout the Mediterranean regions of Southern European.

However, the model presented here does not intend to predict real fire spread or behaviour, but is rather concerned with the functional connectivity of fuel scenarios at regional scales. This said, our argument is that  $T_{\text{pot}}$  is an indirect, consistent and valid estimate for the resistance offered by a single landscape cell towards the propagation of fire: the longer it potentially takes an advancing fire front to cross a landscape cell, measured as potential transit time  $T_{\text{pot}}$ , the higher the resistance and the higher its assigned friction value. In this line, and to emphasize the fact that we interpret the  $T_{\text{pot}}$  values as friction values and use them for the calculation of cost-distance surfaces, they remain unit-less and we refer to them by the denomination ‘potential’. Using this approach for coding the friction layer has several advantages. Its calculation is consistent and unbiased for every landscape cell and is independent of the operator. But the main advantage is that with this approach, the main factors of fire spread can be merged into a single friction value, correctly weighting them depending on their respective level of influence using a widely tested and applied methodology in fire ecology and fire modelling (see for examples Keane et al., 1998, 2000; Russell and McBride, 2003; Stratton, 2004; Fernandes and Botelho, 2004; Duguay et al., 2007). Since all implicit landscape features which influence fire spread are accounted for and quantified, the resulting cost-surfaces convey functional connectivity on a region-wide scale. And indeed, any available approach to calculate the  $\text{ROS}_{\text{max}}$  of an advancing fire front can be considered as suitable, whether a semi-physical/semi-empirical or a strictly physical and multiphase approach is used. This choice will generally depend on data availability and familiarity with any method of estimating  $\text{ROS}_{\text{max}}$ . A recent overview of available fire behaviour and modelling methods and approaches is given for example by Morvan et al. (2004).

### 2.3.2. Fractal estimation of functional connectivity

The geometric complexity, or roughness, of the resulting cost surface can be used as an estimator of connectivity because the more complex a cost surface is, the more deterministic will be its effect on fire propagation. If connectivity for fire propagation is low across the landscape, the resulting cost surface will have a rugged topography, with a coarse spatial structure in relation to the spatial structure of fire propagation. If connectivity is higher, fire spread across the landscape is a more uniform process resulting in a cost surface with less accentuated and generally smoother topography. Fig. 3 provides an example of the low moisture friction surface and one of the resulting cost-distance surface in a three-dimensional perspective. Note that connectivity is a strictly spatial attribute which depends on cost differences as a function of the distance between locations, not on absolute cost values at a single location. For example, a large patch of a single fuel model that is less fire prone and on gentle hill slopes will have homogeneously high friction values, which in turn will generate a large and smooth hump in the cost-surface forming a kind of mesa shape. This reflects that, in those conditions, fire would propagate steadily, albeit slowly because of the high landscape resistance, but the propagation process itself would be spatially homogeneous nonetheless. Therefore, the approach developed in this study makes an explicit distinction between the non-spatial component – quantified by a cost surface’s overall mean cost – and the spatial component – the cost-surface roughness – of fire propagation. The former addresses overall means in a lumped form, while the latter addresses spatial heterogeneity. The combined use of these indicators facilitates the comparison of different cost surfaces.

A common way to quantify the spatial complexity of three-dimensional surfaces is the use of the fractal dimension (DF). It has been widely used to assess the roughness of topographic surfaces and profiles (see for example Burrough, 1981; Mark and Aronson, 1984; Klinkenberg, 1992; Klinkenberg and Goodchild, 1992; Xu et al., 1993; Pardini and Gallart, 1998; Helfenstein and Shepard, 1999; Shepard et al., 2001). The advantage of using DF is that it “... indicates the ability of a set to fill the Euclidean space in which it resides, and is the quantitative description for the fractal characteristics of the investigated object” (Xu et al., 1993). DF thus integrates the cost-surface roughness across the whole landscape into one single, intuitive numerical parameter that is conceptually descriptive, easily measurable and suitable at a variety of scales (Leduc et al., 1994; del Barrio et al., 2000) and complies with Hobson’s (1972) recommendation of morphometric parameters (Klinkenberg and Goodchild, 1992). Klinkenberg (1992), building on the work of Mark and Aronson (1984), compared the fractal dimension from 54 DEMs with 24 traditional geomorphometric parameters and showed that DF is capturing some information about surfaces that traditional morphometric surface parameters do not capture. Similar results are reported by Outcalt et al. (1994). Among the several methods to calculate DF, we selected the variogram method as applied by Klinkenberg and Goodchild (1992). They compared several methods and concluded that the variogram method is the most “robust” fractal dimension estimator for topographic surfaces. Based on the assumption that the surface has a statistical structure similar to a Brownian surface, the fractal

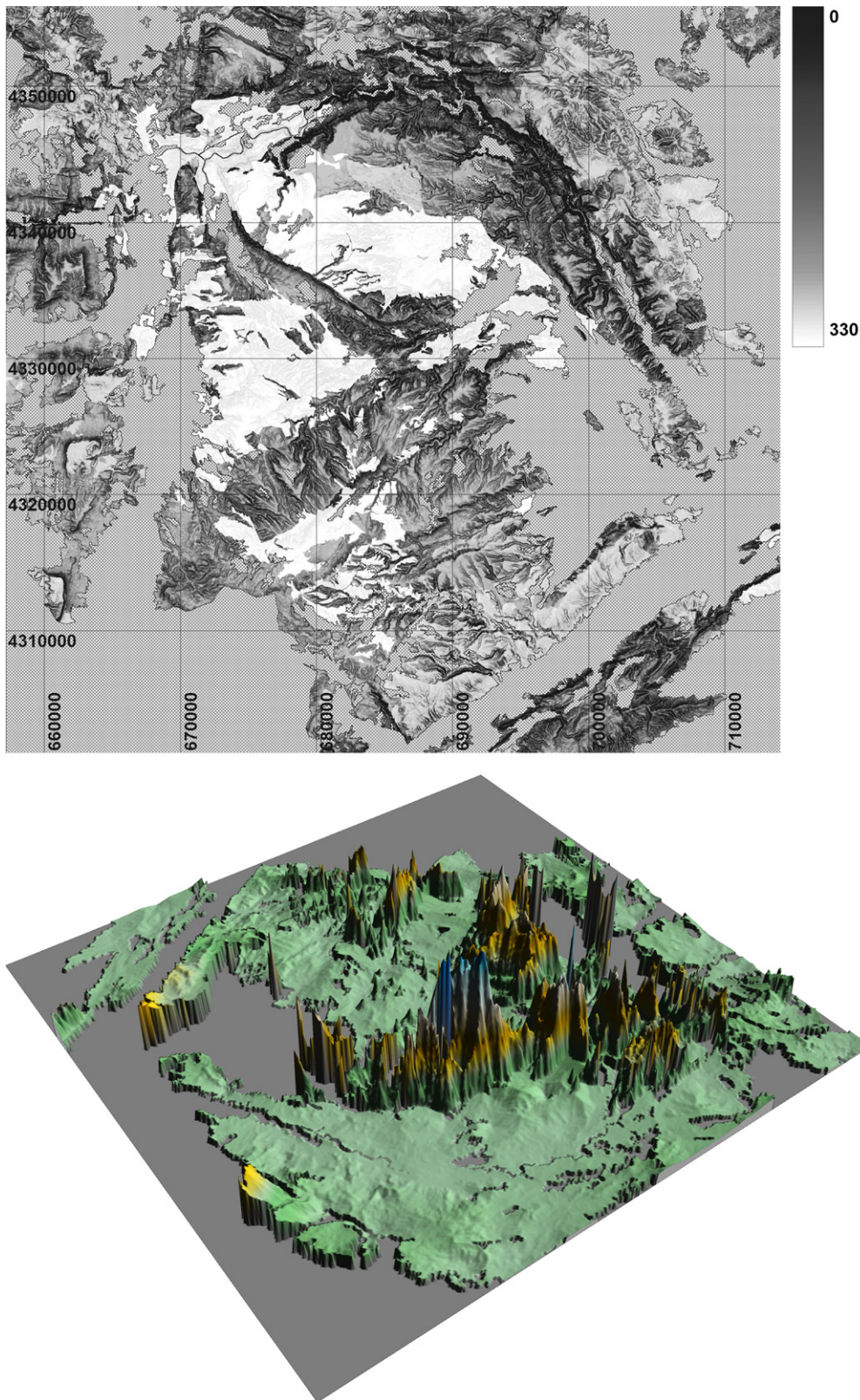


**Fig. 3** – Friction surface for the low moisture scenario (above) and one of the resulting cost-distance surface for 78 ignition points in a 3D perspective. Note how some of the isolated fuel patches have no costs assigned as no ignition points fell within the patch boundaries.



dimension DF can be obtained by the simple relationship.

$$DF = 3 - \frac{1}{2}m \quad (3)$$

where  $m$  is the slope of the best fitted least-squares line to the log–log transformed semivariogram, which in case of statistical self-similarity has a linear form (Burrough, 1981).

The fractal dimension is obtained from the first linear segment of the log–log plot with a coefficient of determination  $r^2 > 0.90$ . The maximum abscissa value of this segment is called the break-distance or scale of fractality and reflects the scale length of fractal structure. Additionally, gamma is the ordinate intercept of the fitted least-squares line and it represents the expected squared difference of values for points a unit distance apart (Klinkenberg and Goodchild, 1992). The data for variogram calculation was obtained by using a sampling network of 10,000 sampling points distributed according to a stratified-random design over fuel-covered areas. Fuel-less areas and isolated fuel patches with no costs assigned (not “ignited”) are automatically excluded from that sampling.

## 2.4. Experimental design

The final aim of our model is the structural analysis of different landscape scenarios and its influence on functional connectivity, not the prediction of dynamic fire behaviour under real environmental conditions. Because of the method used here to quantify landscape resistance towards fire propagation, this can be conveniently accomplished by the re-assignment of different fuel models to vegetation patches and/or superimposing a fuelbreak network, while the general climate conditions can be accounted for as different sets of vegetation moisture contents. Each change can then be simulated by generating a new friction surface to reflect the selected changes and compute a corresponding cost surface. As a previous step, it is necessary to address the problem of the number and spatial allocation of the initial ignition points for cost-calculation.

The experimental test approach outlined in this section was designed specifically with these points in mind (Fig. 4). In a first step, a sensitivity analysis procedure is carried out to identify an optimal number of ignition points and their spatial allocation. It will also enable a preliminary assessment of the influence of the three selected moisture scenarios (low, medium and high), and to evaluate the consistency and stability of the model results. The capability of our model to detect and to quantify changes in functional connectivity across a whole landscape is tested on the second stage of our experimental design, as outlined further below, and is based on different scenarios.

### 2.4.1. Sensitivity analysis

#### 2.4.1.1. Methodology for the selection of initial ignition points.

Imagine a single ignition in the centre of the study area. The resulting cost surface will have a bowl-like shape where accumulated costs increase radially away from the centre, with a pronounced area of low costs in the close vicinity of the ignition point. If a single ignition point was located in the upper left corner, the resulting cost surface, although show-

ing some common patterns with the previous case, like the area of low costs close to the ignition point location and constantly increasing costs radially away, would have a significantly different geometry and range of accumulated cost values. This problem is further aggravated by ignition points that fall within a fuel-less or not flammable area and return an empty cost surface. These three examples clearly demonstrate the pattern inherently linked to cost-surface modelling. In our specific case it leads to the undesired effect of masking relevant cost-surface structures or textural patterns by creating rather homogenous surfaces that do not necessary reflect the landscape’s functional connectivity. We propose to solve this problem as follows.

By increasing the number of ignition points, the deviation in the parameters of the resulting cost surface, specifically the fractal dimension DF, will converge and stabilize beyond a certain threshold, showing only a small range of variation when cost-calculation is repeated several times with the same number of ignition points in different locations. In other words, we seek to maximize the spatial complexity of the resulting cost surfaces up to that point that the spatial complexity is unaltered by the selected ignition points. That way we generate relevant (i.e. non-extreme) cost values for as much of the landscape as possible in any cost surface derived from them. Once this set of *optimal number of ignition points* is identified, the model can be executed with them for simulated changes in fuel configuration or moisture scenarios. The relative differences obtained between a defined reference and a simulated scenario can then be interpreted as changes in functional connectivity that we can attribute to the simulated scenarios.

The first test runs using arbitrary numbers of ignition points with only a limited number of spatial repetitions showed no obvious or detectable trend. We therefore decided to use a step-wise procedure to identify the set with the optimal number of ignition points. We used successive random sets of logarithmically growing densities of ignition points to generate preliminary results, each set consisting of 15 realizations or runs. These repetitions are necessary to ensure the quality of results in terms of statistical variation, and to detect possible outliers and still use sound statistical analysis methods. The parameter trends are visually compared over the whole range of computed sets to encircle the approximate sub-range that contains the *desired set*. In the second step, we use an ANOVA to identify the optimal set within that sub-range that accounts for most of parameter variation of its 15 runs depending on a factor, in this case the moisture scenarios.

We tested a total of 19 sets (see the axis of abscissa in Fig. 7) with 15 repetitions or runs each and at three moisture contents (low, medium and high), such that the model was run 855 ( $19 \times 15 \times 3$ ) times. The number of ignition points selected is of course non-realistic from the perspective of fire behaviour prediction and modelling. But cost surfaces are a representation of connectivity across the landscape, and as such intrinsically different from burning scenarios in a dynamic fire behaviour model. A Monte Carlo approach might be argued in the sense of multiple replications of single ignitions and subsequent computation of corresponding cost-distance surfaces. If this process is repeated often enough, say a 1000 times for example, the problems just discussed could have been possibly mitigated in part. For the scenarios we finally tested (see

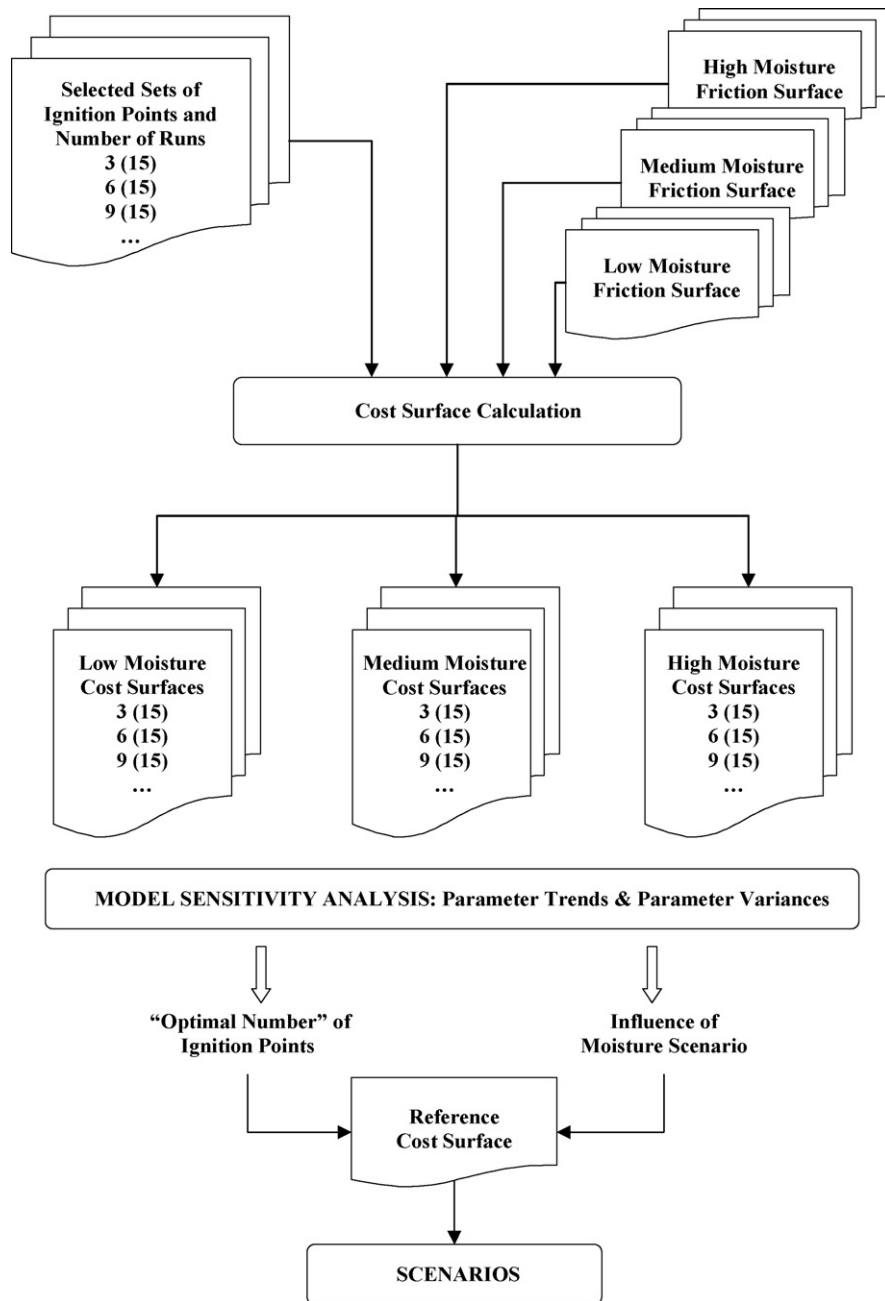


**Fig. 4 – Flowchart of the experimental test approach for selection of the optimal number of ignition points and sensitivity analysis.**

the following section) and at three different moisture sets, we would have to run our model on a total of 24 ( $4 \times 2 \times 3$ ) friction surfaces times one thousand. That would accumulate to a total of 24,000 cost-surface calculations requiring access to serious processing capacities which are seldom available.

**2.4.1.2. Influence of moisture scenarios.** The use of moisture scenarios is conditioned by the requirements of the fire spread model of Rothermel, and for the sensitivity analysis we were forced to use published empirical mean values. Nonetheless, these values can be interpreted as representative of different fire-hazard conditions or for seasonal climate patterns

present in Mediterranean-type ecosystems along a year. Vegetation moisture content greatly influences the fire combustion process and therefore general fire behaviour (Chandler et al., 1983; Pyne, 1984). The influence on the rate of spread of an advancing fire front under different moisture scenarios can be appreciated from Fig. 5. Since the friction value  $T_{pot}$  is a direct function of  $ROS_{max}$  we are able to include this change within our model by using a different friction layer for each specified moisture scenario. If we are able to distinguish between cost-distance surfaces associated to different moisture values, our model would not only serve to assess regional connectivity in general, but also to monitor changes or differences in connectivity in time.

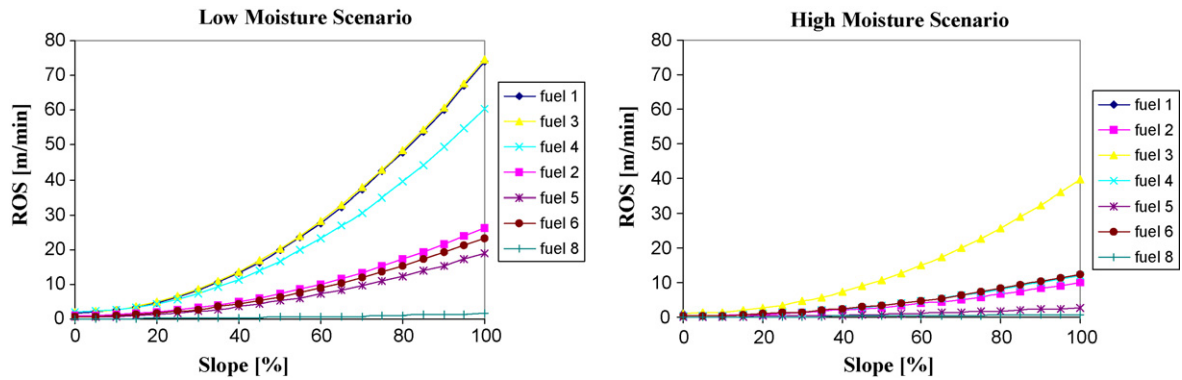


Fig. 5 – Potential rate of spread of the fuel models at low and high moisture content of fuels.

The rate of spread for the different fuel models in the Ayora region under high moisture content decreases greatly compared to the low moisture scenario rate (Fig. 5). Additionally, the differences between different fuel models become blurred or converge to a similar level. Note that fuel model 1 (short grass) is not ignited ( $ROS_{max} = 0$ ) under high moisture conditions, as its dead fuel moisture of extinction of 12% is reached (compare Tables 2 and 3).

#### 2.4.2. Modelling changes in landscape connectivity

The scenario strategy (Fig. 6) is to replace in our reference scenario the fuel model 4 (chaparral) in the fuel layer, a fast fuel where fire propagates at high spread rates, successively by the slower fuel model types 5 (brush), 6 (dormant brush) and 8 (closed timber litter). We are aware, that it is highly improbable that Mediterranean shrublands naturally evolve to closed timber litter formations. However, it is unfortunately still possible to observe reforestation projects in Spain by which large patches of *Q. coccifera* and even *Q. ilex* were replaced by dense and coetaneous masses of fast-growing pines or eucalyptus for timber production. Nonetheless, these scenarios do not intend to simulate a plausible vegetation succession in a Mediterranean ecosystem, but instead aim at testing the model sensitivity. The slower spread rates translate into higher resistance or friction values and finally in a decrease of connectivity across the whole landscape. To show that our model is working correctly, it should be able to reflect and detect these changes.

The second scenario set is identical to the above described one, except that this time the fuelbreaks of the Ayora region are included. The network is organized in three fuelbreak orders. The 1st order fuelbreaks are assigned a fixed friction of 3540, the 10-fold of the maximum friction of the Ayora moisture scenario friction surface (354 friction units). The second and third fuelbreaks are assigned fixed frictions of 1416 and 708, respectively, equivalent to 40% and 20% of the first order fuelbreaks in an intent to reflect the relative differences in width under the assumptions that a direct relationship exists between fuelbreak order and effectiveness (friction) and that the fuelbreaks would not really stop a fire but rather slow it down. We assigned the friction values to the fuelbreaks rather arbitrarily in comparison with the sound approach to code the general friction surface of the fuel models. Unfortunately, we are not aware of how we could solve the issue

with the fuelbreak network satisfactorily. Including the network of fuelbreaks this way comes at a significant expense. The scale of friction values is no longer consistent between the scenario sets with and without fuelbreaks, as well as it is not consistent between the three fuelbreak orders. As a direct consequence, the absolute values of the scenario parameters with and without fuelbreaks are not directly comparable anymore in a quantitative sense. For the same reason, we refrain from trying to quantify or interpret the influence of the different fuelbreak orders separately on their own, but consider the network as a single landscape feature.

## 3. Results and discussion

### 3.1. Sensitivity analysis

The results of the sensitivity analysis for the three fractal parameters, as well as for the mean costs of the cost surfaces as a lumped, non-spatial estimate of the overall cost, are shown in Fig. 7.

The mean costs show the most constant trend among the four parameters, steadily decreasing with increasing numbers of ignition points. The larger the ignition point densities, the shorter the average cost-distance from any cell to its nearest ignition point. The differences between the three moisture scenarios reflect the general growing friction values associated with increasing moisture content of fuels. In general, the differences between moisture scenarios diminish with decreasing mean cost to finally nearly disappear when the point density reaches maximum values. This indicates that, under extreme circumstances when fire density is very high, the differences in frictions loose much of its influence on fire propagation over the whole landscape. Apparently, differences between low and high, and between medium and high moisture scenarios is visible, though between the low and medium moisture scenario they become less pronounced with higher point densities.

Break distance  $B$  or the scale of fractality shows a similar decreasing trend with growing point density. A central range is visible with a steady and smoother decreasing trend, but within it no evident distinction is possible between the three moisture scenarios. The sets with fewer ignition points, though also showing a general decreasing trend, seem not to

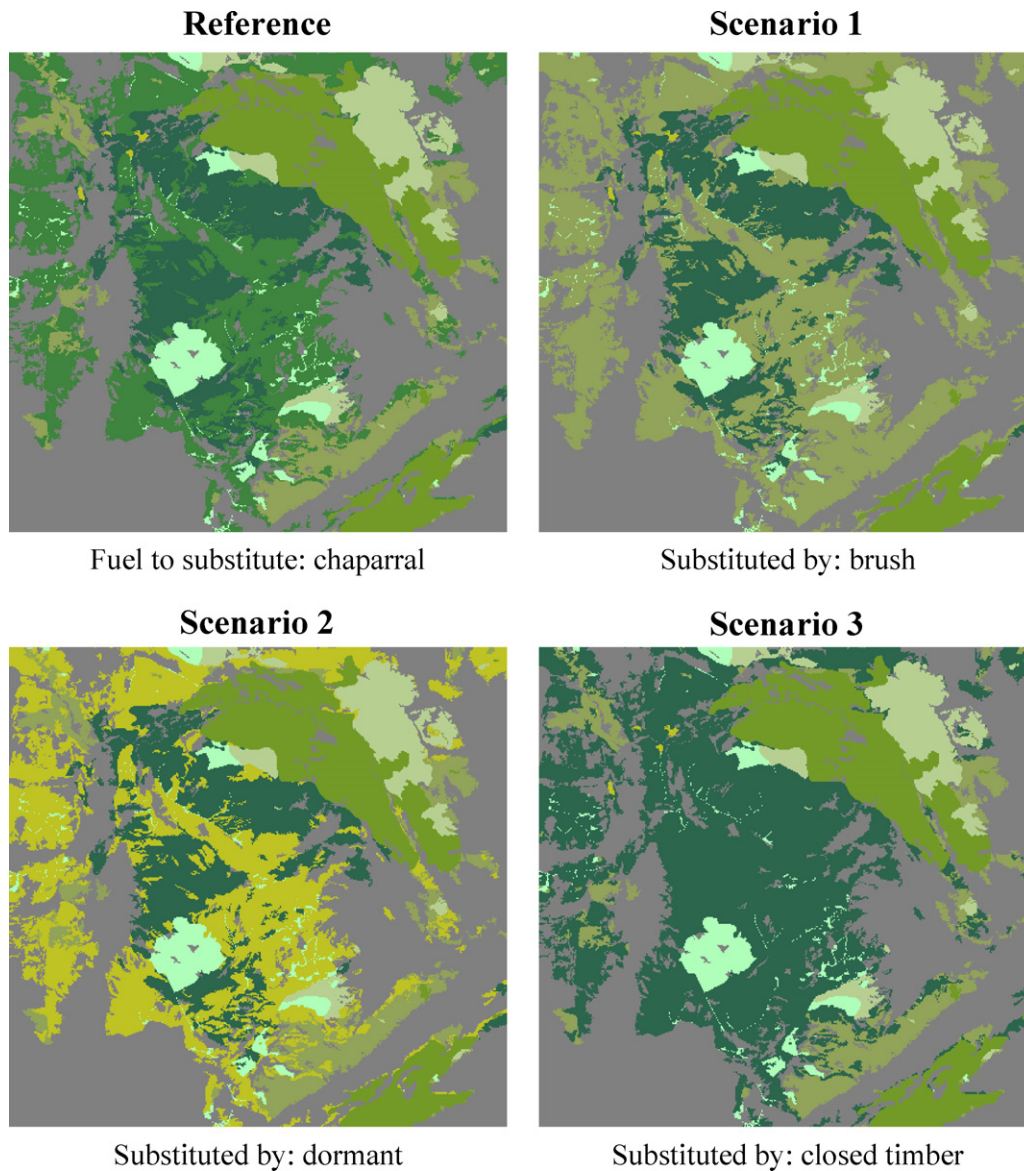


**Fig. 6 – Ayora scenarios without fuelbreaks. The Ayora fuelbreak scenarios differ only in the additional fuelbreaks included. The spatial distribution of the fuelbreaks can be appreciated in Fig. 1. The legend (not shown here) is identical to the legend given in Fig. 1.**

follow any recognizable pattern whereas at high point densities the values start to diverge.

By comparison, the fractal dimension  $DF$  shows an inverse trend.  $DF$  values increase with growing point density, but again a similar general three-part structured pattern is apparent. The central range, between the sets of 30 and 330/534 ignition points, shows a monotonous increase and very modest differences among moisture scenarios. To the left and right of this central range,  $DF$  becomes less stable with increased differences between the moisture scenarios. This progression reflects, like the decreasing mean costs, the overall growing connectivity induced by the high density of spread points across the friction surface. As fewer ignition points create a coarse structure with only few local minima, the resulting cost topography centered around them spans across the whole landscape, but with little local variation, and generally high

cost values for each landscape cell. The increase in ignition point density creates more local minima evenly distributed across the landscape which results in a cost-surface topography characterized by a finer texture, albeit with generally lower costs for each cell.

Using a more figurative description: low ignition point densities create a coarse-scale cost topography with low space filling capability in three-dimensional space despite its high overall mean costs, and thus the lower fractal dimension. Whereas a high point density creates a cost topography at a finer-scale, though generally with much lower mean costs, which translates into a higher space filling capability and thus a higher fractal dimension.

The finer the texture of the cost-surface topography, the smaller the break distance or scale length needed to detect and to measure its fractal structure, whereas with coarser

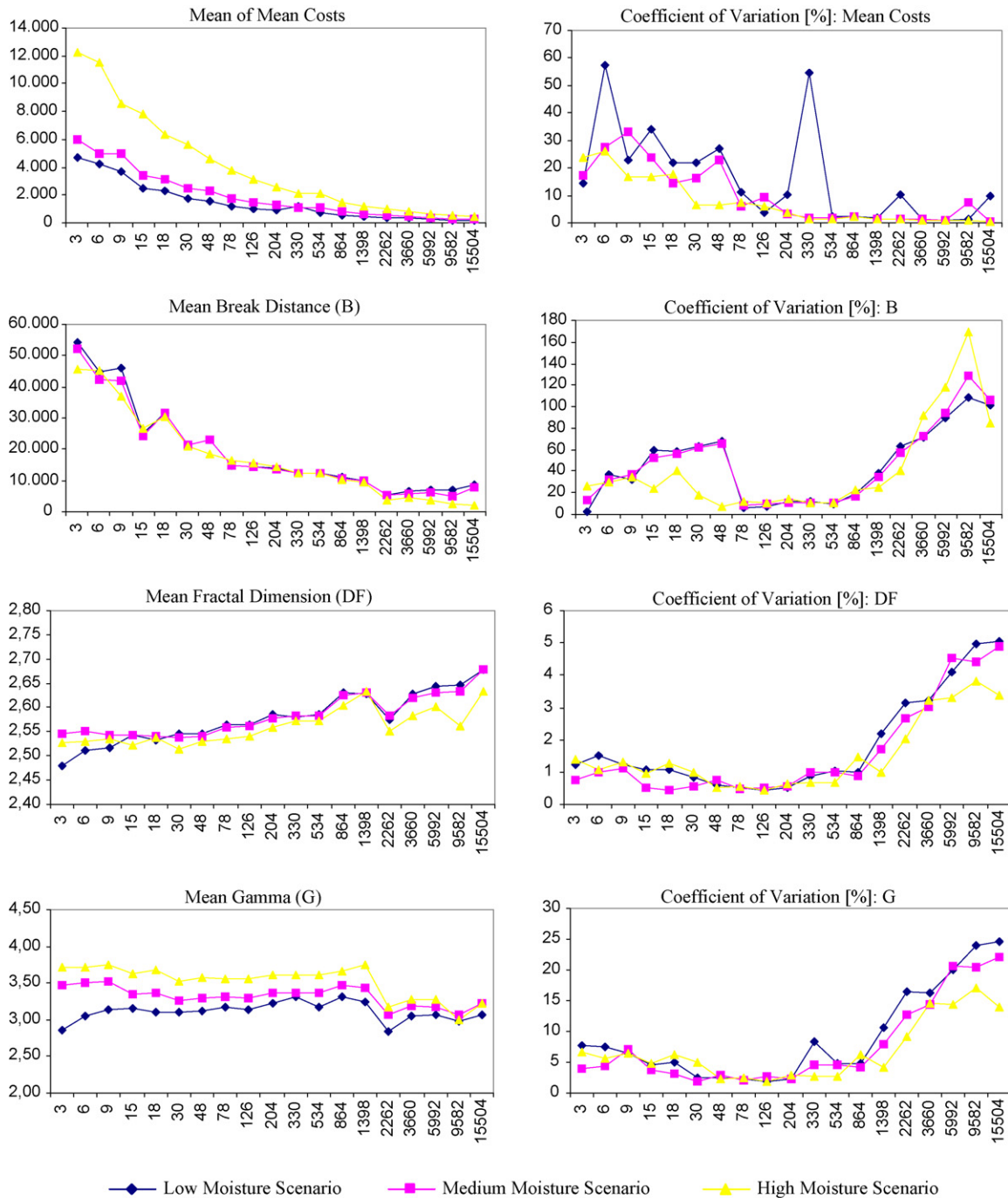


**Fig. 7 – Results of the sensitivity analysis. The sets with their number of ignition points are on the abscissa. Values are mean values based on the 15 runs per set (left) and their respective coefficients of variation (right) for the extracted parameters mean costs, break distance (B), fractal dimension (DF) and gamma (G).**

texture a larger break distance is necessary. If one would use inappropriate break distances for these kind of surfaces, where fractality occurs only within a limited spatial range of length scales, surfaces would look smooth and feature-less.

In general, the mean values of the gamma parameter G for the sets of the moisture scenarios seem to stay constant and to keep the relative differences between the moisture scenarios,

especially in the central range. The rather constant values over the whole range of ignition point sets make gamma look much like a spatial noise.

To compare the magnitude of variation within the different sample sets, we use the coefficient of variation (CV). It is expressed in a percentage ratio and allows to compare data samples with greatly varying standard deviation and mean values (Sachs, 1982; Sokal and Rohlf, 1995).

The coefficient of variation of the mean costs shows no apparent pattern, with sudden jumps especially for the sets below 78 ignition points and again at set 330. But in general terms, the CV of mean costs reaches low levels with increasing ignition points.

For the spatial parameters DF, B and G the general three-part pattern becomes now clearly visible. The central range between sets of 30 and 204 or 330 ignition points have the lowest overall CV, with the exception of B, for which the stable section clearly starts with a sharp drop between sets 48 and 78. But as a general pattern for the three spatial parameters, with increasing ignition points the variation increases to reach differences in CV several times greater than their respective central section. The same is apparent for the sets below 30 or 48 ignition points for fractal dimension and gamma, though here the variation does not reach values as high as observed with high ignition point densities.

Though it was initially supposed that, in general, parameter variations would show a decreasing trend as ignition point density is increased, only the mean of the cost surface, the non-spatial, statistical parameter, follows this hypothesis. All the spatial parameters display a common, more or less coinciding, range with a relatively stable pattern within a fractal scale length B between 10,000 and 20,000 m and is associated with the sets between 20/48 and 204/330 ignition points and with respective DF values between 2.525 and 2.575. We interpret that this stable segment is caused by a spatial tune between the spatial structure of the landscape friction as parameterized for this particular case, and the spatial density of ignition points. For that reason, the algorithm sensitivity to fuel moisture is searched within this interval.

As the optimal number of ignition points should be characterized by robust, consistent and reliable mean values for the fractal dimension based on the 15 repetitions – the most important spatial parameter of the cost-distance surfaces – we apply a one-way ANOVA to the sets 30–204 using the three moisture scenarios as the independent factor (Table 4). To

identify the set where most variance is explained we use the partial ETA squared value (Bahrenberg et al., 1992). The prerequisites for a reliable ANOVA – normal distribution and equal variance among groups – were tested with Shapiro-Wilk and Levene's test, respectively.

Differences among the three moisture scenarios are statistically significant for all sets with significance values  $p \leq 0.001$ , except for set 48 with  $p = 0.012$ . The factor moisture scenario accounts most for data variance at set number 78 where the partial ETA squared value is 0.518. The Scheffe's post hoc test for this set reveal that in fact, only the high moisture scenario is statistically significant from both low and medium moisture scenario, while low and medium moisture scenario values show no statistically detectable differences. This is most likely due to fuel model 8 (closed timber litter) which covers nearly 20% of the total fuel area, but does not ignite at high moisture values and is therefore excluded from sampling.

Since no statistically significant difference can be detected between low and medium moisture when directly compared, the conclusion is that with the optimal number of ignition points selected – set 78 – the influence of the moisture content can not be assessed for lower levels of vegetation moisture contents. Also, as a practical conclusion, and since both scenarios can not be distinguished from each other, nothing speaks against using Ayora specific moisture values for the scenario test procedure as the Ayora moisture values lie between the low and medium moisture scenario values.

### 3.2. Scenario modelling

The results of the Ayora and Ayora fuelbreak scenario sets (denoted with fb) are displayed in Table 5 and in Fig. 8. Gamma values are not included in the table. We decided to exclude this parameter as in the course of the sensitivity analysis it became evident that gamma does not provide interpretable information about cost surfaces.

**Table 4 – Summary table for the one-way ANOVAs for the selected sets of ignition point numbers**

| Factor: moisture scenario | Number of ignition points | Dependent variable: mean DF | d.f. | F      | Sig.  | Partial ETA squared | Homogenous subsets |
|---------------------------|---------------------------|-----------------------------|------|--------|-------|---------------------|--------------------|
| Low                       | 30                        | 2.545                       | 2    | 8.744  | 0.001 | 0.294               | B                  |
| Medium                    |                           | 2.537                       |      |        |       |                     | B                  |
| High                      |                           | 2.514                       |      |        |       |                     | A                  |
| Low                       | 48                        | 2.547                       | 2    | 4.906  | 0.012 | 0.189               | B                  |
| Medium                    |                           | 2.540                       |      |        |       |                     | B                  |
| High                      |                           | 2.529                       |      |        |       |                     | A                  |
| Low                       | 78                        | 2.566                       | 2    | 22.605 | 0.000 | 0.518               | B                  |
| Medium                    |                           | 2.558                       |      |        |       |                     | B                  |
| High                      |                           | 2.535                       |      |        |       |                     | A                  |
| Low                       | 126                       | 2.565                       | 2    | 16.131 | 0.000 | 0.434               | B                  |
| Medium                    |                           | 2.561                       |      |        |       |                     | B                  |
| High                      |                           | 2.541                       |      |        |       |                     | A                  |
| Low                       | 204                       | 2.584                       | 2    | 12.160 | 0.000 | 0.367               | B                  |
| Medium                    |                           | 2.577                       |      |        |       |                     | B                  |
| High                      |                           | 2.559                       |      |        |       |                     | A                  |

Homogenous subsets as given by the Scheffe post hoc multiple comparison range test.

**Table 5 – Results of the modelled scenarios**

| Ayora scenario                | Mean costs |      |     | Break distance (B) |      |      | Fractal dimension (DF) |          |     |
|-------------------------------|------------|------|-----|--------------------|------|------|------------------------|----------|-----|
|                               | Mean       | S.D. | CV  | Mean               | S.D. | CV   | Mean                   | S.D.     | CV  |
| Reference                     | 1399       | 73   | 5.2 | 14,933             | 1280 | 8.6  | 2.561453               | 0.013746 | 0.5 |
| 1                             | 2088       | 127  | 6.1 | 15,200             | 1897 | 12.5 | 2.546520               | 0.014377 | 0.6 |
| 2                             | 1755       | 102  | 5.8 | 15,133             | 1642 | 10.8 | 2.554173               | 0.014914 | 0.6 |
| 3                             | 4939       | 160  | 3.2 | 13,929             | 1439 | 10.3 | 2.518107               | 0.015198 | 0.6 |
| Ayora fuelbreak scenario (fb) | Mean costs |      |     | Break distance (B) |      |      | Fractal dimension (DF) |          |     |
|                               | Mean       | S.D. | CV  | Mean               | S.D. | CV   | Mean                   | S.D.     | CV  |
| Reference (fb)                | 2964       | 210  | 7.1 | 20,133             | 3091 | 15.4 | 2.655380               | 0.011061 | 0.4 |
| 1 (fb)                        | 3752       | 232  | 6.2 | 19,800             | 2933 | 14.8 | 2.644993               | 0.014931 | 0.6 |
| 2 (fb)                        | 3366       | 221  | 6.6 | 20,000             | 3117 | 15.6 | 2.650800               | 0.013441 | 0.5 |
| 3 (fb)                        | 7076       | 285  | 4.0 | 18,143             | 2656 | 14.6 | 2.588364               | 0.016894 | 0.7 |

Statistics given for the extracted parameters mean costs, break distance (B) and fractal dimension (DF) of the Ayora scenario and Ayora fuelbreak scenario (fb).

Two aspects are apparent from a first look in Fig. 8. First, the parameters of both scenario sets display identical patterns in their within set differences between the three scenarios and their respective reference. And second, the scenarios

with fuelbreaks are on higher absolute value levels than their corresponding counterpart without fuelbreaks. We will first concentrate on the former aspect.

As expected, the mean costs for all three scenarios are higher than the reference costs since the chaparral fuel was substituted consecutively by slower fuels. The highest mean costs displayed in scenario 3 correspond to the slowest of all three fuel types used in the replacement, the lesser costs in scenarios 1 and 2 are matched by the smaller differences in spread rates of the corresponding fuel models.

Fractal dimension values (DF) are inversely proportional to the mean costs, as we could already observe during the sensitivity analysis. The largest difference between the reference and a scenario value is again found at scenario 3. While the fractal dimensions of scenarios 1 and 2 are also smaller than the reference value, the differences between both appear to be minimal.

The break distance (B) seems not to be affected by the changes made, though a minimal decrease in break distance seems to be the case in scenario 3.

Again, a one-way ANOVA is applied to the three parameters as dependent variables and the scenario set as independent factor. The results are presented in Table 6. While no statistically significant difference can be detected between break distances the differences in mean costs are highly significant ( $p < 0.001$ ). Scheffe's post hoc test clearly separates all scenarios from the reference and from each other.

The ANOVA for fractal dimension values also detects statistically significant differences among the scenarios ( $p < 0.001$ ). Scheffe's post hoc tests can detect only differences between scenario 3 and the others, but not among them.

In summary, this statistical analysis reveals that the changes made by substituting fuel model 4 (chaparral) with slower fuel models attract significantly higher mean cost for fire spread across the landscape. In addition to that, the largest change in the generated cost-surface structure is found in scenario 3, where fuel model 8 (closed timber litter) was included. If we concentrate on the clearly different situations the reference scenario and scenario 3 represent, we can facilitate the interpretation of these results.

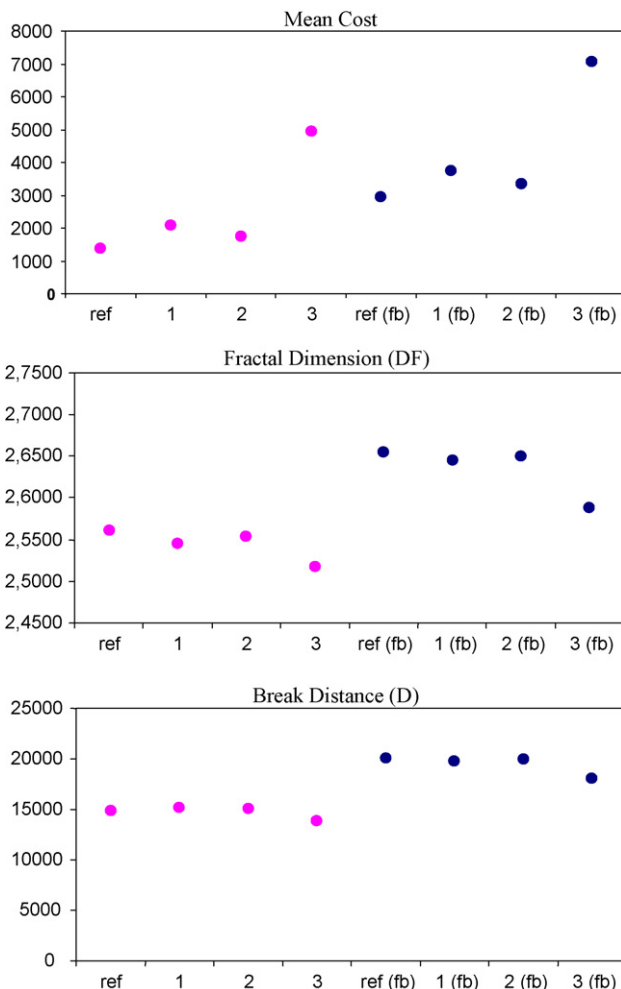


**Fig. 8 – Results of the Ayora scenarios on the left and Ayora fuelbreak (fb) scenarios on the right.**

**Table 6 – Summary table for the one-way ANOVAs for the Ayora scenario without fuelbreaks**

| Factor: fuel scenario | Number of ignition points | Dependent variable: mean DF    | d.f. | F        | Sig.  | Partial ETA squared | Homogenous subgroups |
|-----------------------|---------------------------|--------------------------------|------|----------|-------|---------------------|----------------------|
| Reference             | 78                        | 2.561                          | 3    | 24.328   | 0.000 | 0.570               | A                    |
| 1                     |                           | 2.547                          | 3    |          |       |                     | A                    |
| 2                     |                           | 2.554                          | 3    |          |       |                     | A                    |
| 3                     |                           | 2.518                          | 3    |          |       |                     | B                    |
| Factor: fuel scenario | Number of ignition points | Dependent variable: mean B     | d.f. | F        | Sig.  | Partial ETA squared | Homogenous subgroups |
| Reference             | 78                        | 14,933                         | 3    | 1.987    | 0.127 | 0.098               |                      |
| 1                     |                           | 15,200                         | 3    |          |       |                     |                      |
| 2                     |                           | 15,133                         | 3    |          |       |                     |                      |
| 3                     |                           | 13,929                         | 3    |          |       |                     |                      |
| Factor: fuel scenario | Number of ignition points | Dependent variable: mean costs | d.f. | F        | Sig.  | Partial ETA squared | Homogenous subgroups |
| Reference             | 78                        | 1399                           | 3    | 2635.758 | 0.000 | 0.993               | A                    |
| 1                     |                           | 2088                           | 3    |          |       |                     | B                    |
| 2                     |                           | 1755                           | 3    |          |       |                     | C                    |
| 3                     |                           | 4939                           | 3    |          |       |                     | D                    |

Homogenous subsets as given by the Scheffe post hoc multiple comparison range test.

The reference scenario stands for a high fire-risk situation. Large areas are covered with fuel model 4 which is associated to the typical dense shrublands dominating the Ayora region with ca. 40% of the total fuel covered area, and is characterized by highly flammable fuels and high fuel loads. These shrublands are widely distributed across the whole landscape in patches of different sizes partly interwoven and bordering with many patches of other fuel types (see Fig. 6). Fire spreads at ease with high spread rates across the landscape, which is expressed through the lower mean costs of the reference situation when compared to the three tested scenarios, but specially when compared to scenario 3. Each time the fire spread crosses into a patch with a different fuel type, irregularities are induced onto the cost surface at the boundaries between two adjacent patches as the overall friction values change according to the fuel model and the associated friction of the new patch. These local, line-shaped irregularities create a fine-scale textured topography which is reflected in the relatively higher fractal dimension.

The situation in scenario 3 is the lowest fire-risk situation included in the scenario procedure. Fuel model 8 (closed timber litter) stands for well-developed forest stands with little understory and much lower fuel loads and spread rates. As fire encounters more resistance when spreading across this fuel type, the increase in costs is very high. A significant part of the region is covered by this fuel type, somewhat concentrated on the central parts in few relatively large patches, which are more or less surrounded by fuel model 4 (chaparral) (see Fig. 6). By substituting all the chaparral patches by closed timber litter, the percentage of total area now covered by this fuel model is raised from 19.2% to nearly 60% becomes the dominating fuel in the region. And if we keep in mind the spatial neighbourhood relationship between the patches of both fuel types, in the process of substitution an apparent different spatial arrangement of fuels is created. Not only has the total area covered by fuel model 8 increased dramatically,

but now fuel model 8 (closed timber litter) is concentrated in what could be described as one single homogenous and continuous fuel patch. When fire spreads across the landscape under this spatial setting, it encounters this large contiguous patch of a high resistance to fire spread, and the mean cost increases significantly. But the spreading process itself is steady and homogenous across a wide extent of the landscape since changes in fuel type are now less likely. The cost topography of the surfaces resulting from this spatial arrangement of fuels display a large high-cost mesa shape extending over much of its central area. Since this cost mesa is in general characterized by a very homogenous texture with little local irregularities its space-filling ability is not really increased at the current extent of the study region. This phenomenon is what causes the lower fractal dimensions of the cost-distance surfaces of scenario 3.

The first impression gained at the beginning, that the general pattern of within set differences is identical in the sets with and without fuelbreaks, is confirmed by the ANOVA and the Scheffe post hoc tests applied to the results of the Ayora fuelbreak scenarios. That is, we find again statistically significant differences among all scenarios in their surface mean costs ( $p < 0.001$ ). And again, only the scenario 3(fb) has a significantly different spatial cost structure reflected by the fractal dimension value ( $p < 0.001$ ), while scenarios 1(fb) and 2(fb) show no apparent change in their spatial structure. Since these results are identical, the corresponding tables are not presented neither discussed here. Though the Ayora and Ayora fuelbreak scenarios cannot be compared directly with each other due to the friction scale inconsistency introduced by the arbitrary way the fuelbreaks were coded, some important conclusions can be drawn from the results.

The interesting and really important point is the fact that the parameter values in the Ayora fuelbreak scenario are increased by what seems to be a constant value when we compare them to their corresponding scenario without fuel-



breaks. Of course this constant value is directly associated to the friction values assigned to the fuelbreaks. If the assigned frictions were higher or lower than those based on the 10-fold of the friction maximum, the constant off-set would certainly be higher or lower respectively than the one observed in the results. But the point here is, that whenever fuelbreaks are included, this off-set like increase in parameter values would always be observed. Thus, as the underlying friction surface or landscape structure is identical between the two scenario sets – except for the fuelbreaks – this off-set increase is the direct influence of the fuelbreak network when present in the landscape. The magnitude of the influence of the fuelbreak network on the landscape becomes clearly evident when we keep in mind that fuelbreaks account only for 0.8% of the total fuel cover, while the differences displayed between the reference scenario and scenario 3 involved substituting nearly 40% of the total fuel cover by a less fire-prone fuel model. So, although fuelbreaks only account for very small part of the total area the impact caused has an impressive result on the spatial structure of the cost surface. The influence of the fuelbreaks is displayed in both the mean costs and the fractal dimension of the cost surfaces.

When crossing the fuelbreaks a local line-shaped irregularity is induced along the whole fuelbreak network, a kind of contiguous high-friction ridge spanning across the surface. This is much like the effect of crossing into patches of different fuel types, but with much higher local costs involved since fuelbreaks offer a higher resistance. This friction-ridge leads to an increase of the spatial heterogeneity impeding homogeneous and constant fire spread across the landscape, which is reflected by the increase in the fractal dimension of the cost surfaces. While this effect is restricted locally to the fuelbreaks, the landscape wide increase in resistance towards fire propagation is evident in the mean cost of the respective surfaces. Both combined effects of fuelbreaks seem to be more effective in mitigating the general fire-prone character of a landscape than substituting even large patches of fast fuels by significantly slower fuels. At this point it is convenient to stress that only the contribution of the landscape structure is being discussed, and that simulations of real fire events under dynamic conditions might lead to a different result.

If a fuelbreak network is planned, it should be carefully designed to adapt to the local landscape with fuelbreaks placed along “hot-spots” for fire propagation like between fast fuel areas or parallel along roads to maximize the impact on fire propagation and minimizing the visual impact onto the landscape.

But the general conclusion from this scenario analysis is that connectivity for fire propagation may be impeded substantially by increasing the spatial heterogeneity of the fuel matrix and shifting it to a finer texture (i.e. decreasing its scale length or ‘up-scaling’ the landscape). Since crossing into fuel patches of slower fuel types has a similar impact, though of a lesser magnitude, it is recommendable to plan for patches of slow fuels interspersed across the landscape. Such scale dependency between fuel load grain and fire spread was also found by Kerby et al. (2007). Placed strategically in between fast fuels or in their close vicinity, the resulting heterogeneity is the real crucial factor to slow down fire spread, rather than the effect of fire resistant fuel patches by themselves. Finney

(2001) found also that certain treatment patterns reduce the spread rate over the whole landscape, even outside the treatment units where the fire was forced to flank. One advantage of the model presented in this work is that both the intrinsic resistance and the spatial arrangement (size and interspersion) of fuel patches associated to candidate scenarios can be assessed explicitly in terms of their respective contributions to the connectivity of fire spread.

Since “replacing” fast fuels by slow fuel types involves major changes in vegetation cover, those measures have to be carefully planned ahead and executed since the time scale involved extends to the order of one or two decades and do not come into effect for a long time until the forest stands are well developed. Nonetheless, local fuel thinning measurements and controlled grazing activities to keep fuel load constantly low in critical and strategic important areas with a controlled spatial arrangement as suggested above, would yield a more “natural” and integrated fuelbreak network which can be implemented and maintained in fire-prone landscapes.

Though this kind of recommendations are already known under the terms of shaded fuelbreak concepts (Agee et al., 2000) and preventive silvi-cultural forest management (Gonzalez Rebollos et al., 1999; Velez, 2000b), converging to them using our approach to regional connectivity implemented here shows its own potential, with the additional advantages of standardized input data, automatic computation, and generating output results in cartographic (GIS) format.

## 4. Concluding remarks

This work presents a new approach to assess the structural contribution of a landscape to fire propagation. It is based on the estimation of connectivity through cost-distance surfaces. The basic steps are: (i) coding of an existing fuel distribution map to friction, as the time required by fire to cross every cell at the working resolution; (ii) specification of a network of simulated ignition points from which cost-distances will be computed, in terms both of spatial pattern and number of simulations required to build a statistical distribution; (iii) modelling of cost surfaces for each realization of the ignition points network; (iv) computing the fractal dimension of individual cost surfaces as a descriptor of their spatial complexity; (v) using the statistical distribution of fractal parameters to estimate the landscape connectivity for fire propagation. Results from this approach suit particularly well to relative comparisons among different scenarios of fuel distribution and properties. Some of its steps involve important decisions and assumptions that are summarized below for a general application of the approach.

### 4.1. Calculation of friction surfaces

The friction values were assigned based on existing and accepted methods from fire behaviour prediction modelling. By coding the friction surface using the potential transit time  $E_{pot}$  through any given cell, we can account for some of the major factors influencing general fire behaviour known as the fire-triangle: slope as topography factor, vegetation for-

mations as NFFL standard fuel models, and general climate conditions as different sets of vegetation moisture contents. This way our approach becomes spatially explicit. Moreover, we obtain a consistent, unbiased and repeatable scale for friction values, making it unnecessary to identify weighting coefficients for the different input factors to merge them into one single friction surface.

The NFFL standard fuel models were developed for vegetation formations in the USA and did not aim at being representative of the vegetation structure in other parts of the world. This is true too for the study area used in this work, and as a result the parameterization used here may not reflect properly the actual response of that landscape to fire. Nevertheless, this kind of fuel models make an acknowledged need for fire management in landscapes and adaptations have been developed for many areas including Mediterranean Spain (see cited literature in the preceding section on data sets), and new methods to devise them are being rapidly evolved (Velasco, 2000; Riaño et al., 2001, 2002). Their use as input data in modelling approaches such as that discussed here only stresses their potential and the urgent need to develop sources of parameterized information on the landscape.

Still, an unbiased and objective method for coding of the fuelbreak's friction values has to be found to enable us to include the effect of fuelbreaks consistently with the friction scale applied to the landscape. Of particular interest is the inherent difficulty of representing linear and narrow features in a raster format, and especially the typical width of these features with respect to the working raster resolution.

#### 4.2. Selection of initial ignition points

To overcome or at least to minimize the fragmentation effect induced by the spatial arrangement of fuels, which may appear in patches surrounded by non-burning areas, a simple but effective calibration approach was developed. The model aims at the structural analysis of landscape scenarios rather than the dynamic simulation of concrete fire events over it. Therefore, the objective of this calibration is to set a number of random and simultaneous ignition points that optimizes the generation of relevant cost values for as much territory as possible in any cost surface. This is technically defined as maximizing the spatial complexity of the resulting cost surfaces. Too many or too few points will result in cost surfaces with very small or very large values, respectively, any of which possibilities creating rather homogeneous textures that are unsuitable to assess connectivity. The practical outcome is that the number of cost surfaces required to show significant differences among scenarios is greatly reduced, as it is the required computing time compared with other possible approaches to the selection of suitable ignition points. Successive random sets of logarithmically growing densities of ignition points are used to generate preliminary results. Each set consists of 15 realizations or runs that are necessary to ensure the quality of results in terms of statistical variation and to detect possible outliers and still use sound statistical analysis methods. Those sets serve to assess the general model response and simultaneously to find the optimal number of ignition points for further application. As this number is fine-tuned to the sources of spatial variation of the

input data, when including new data of different spatial characteristics it is necessary to repeat the calibration procedure. Finding a formal relationship between the spatial structure of a given fuel scenario and the optimal density of ignition points would greatly benefit this approach by reducing significantly the time consuming calibration procedure and making it possible to directly compare results from different regions.

#### 4.3. General model performance

The general performance of our approach is satisfactory and promising. During the sensitivity test procedure, it yielded results consistent with what could be expected.

The mean costs decreased clearly with growing point density, while the fractal dimension captured the changes in cost topography complexity. The break distance or scale of fractality evolved consistent with the fractal dimension values, reflecting the change in scale needed to detect the fine-scaled surface texture at higher numbers of ignition points. The gamma values exhibited a noise-like constant progression at specific values, but no real change was apparent, leading to the conclusion that this parameter does not provide any helpful or interpretable information about these cost surfaces.

This part of the model may be used in other ecological models. In more general terms, the use of a fractal approach to assess changes in the spatial heterogeneity of a response surface, such as cost surfaces in this work, ensures a consistent and explicit method to account for the impact of a given driver on the spatial scale of the resulting pattern. For example, the impact of climate change scenarios on the distribution of a certain species has been assessed in terms of changes in the fractal dimension of the associated suitability surfaces fitted using climatic variables as predictors (del Barrio et al., 2006).

The model is apparently sensitive to broad changes in moisture contents as the results at both extremes of point densities showed some visible differences. However, within the range of results from which the optimal number of ignition points was selected, the model was not able to detect statistically significant differences between moisture values in the drier end of the scale.

We successfully distinguished during the scenario tests between situations of different fire-hazard levels and the results in mean costs and the fractal dimension were interpretable. Furthermore, though we used rather arbitrary friction values as approximation to include the presence of fuelbreaks, we were still able to interpret the results from the fuelbreak scenario sets.

In this study we used an isotropic cost algorithm for cost-distance calculation, not distinguishing between up-hill and down-hill fire spread. As the down-hill rate of spread significantly decreases on down-hill fire spread (Van Wagner, 1988), we thus overestimate in general the cost-distances. Though this overestimation still enables a direct comparison of different scenarios, the implementation of an anisotropic cost algorithm would result in a finer and more realistic cost-surface structure. In fact, except for Michels et al. (2001), none of the cited studies makes an explicit difference between up-hill and down-hill movements all using isotropic cost algorithms of some sort. Depending on data resolution and the movement process in question, the application of an

anisotropic algorithm might not always be necessary to carry out a cost-distance analysis. But the explicit directional distinction accounted for by an anisotropic cost algorithm gains more and more importance with higher data resolution and specially when investigating the dispersal of contagious disturbances across a landscape.

These findings attest to the operational possibilities of the procedure as a tool for land and forest management. It is easy to implement and can be used to evaluate the structural influence of changes in the vegetation cover on fire spread across the landscape. Additionally, it may provide support to the use of dynamic fire behaviour prediction models by shortlisting alternative landscape scenarios.

From a more general perspective, the approach presented here may involve advances in two aspects of ecological modelling. On one hand, it implements an operational definition of regional connectivity, whereby its structural and spatial components are explicitly isolated. More commonly, connectivity is assessed through the outcome of some dynamic process, either a species population dispersal or, in the analogous case of this work, fire behaviour simulation. As a result, the landscape contribution is treated implicitly and cannot be separated from the process under consideration. On the other hand, the use of fractal dimension and other descriptors of the spatial structure to compare maps of continuous variables may represent a useful procedure for the further use of spatial information, such as scale, in numerical models. It all boils down to the yet unsolved challenge of controlling the spatial dimension, which means not only to enter into the space, but also to be able to get out of it.

## Acknowledgements

This research was supported by the EC GeoRange project (Geomatics in the Assessment and Sustainable Management of Mediterranean Rangelands), contract number EVK2-2000-22089. It was part of the MSc thesis of the author J.R.G. and was developed during a research stay at the Estacion Experimental de Zonas Aridas (EEZA, CSIC) in cooperation with the Remote Sensing Department, University Trier, Germany. J.R.G. is funded by a doctoral scholarship from the Spanish Ministry for Science and Education (MEC-FPI: BES-2005-8691, BOE ORDEN ECI/4484/2004) and the financial support provided for writing part of this manuscript is kindly acknowledged. We would like to thank the CEAM (Centro de Estudios Ambientales del Mediterraneo, Valencia, Spain) for providing the data. Alberto Ruiz (EEZA-CSIC) coded the model software and Maria E. Sanjuan (EEZA-CSIC) kindly helped with the figures and with her expertise in GIS software and data formats. We also wish to thank the anonymous reviewers for their constructive comments which helped to improve the quality of this paper.

## REFERENCES

- Adriaensen, F., Chardon, J.P., De Blust, G., Swinnen, E., Villalba, S., Gulinck, H., Matthysen, E., 2003. The Application of 'least-cost' modelling as a functional landscape model. *Landscape Urban Plan.* 64, 233–247.
- Agee, J.K., Bahro, B., Finney, M.A., Omi, P.N., Sapsis, D.B., Skinner, C.N., van Wagendonk, J.W., Weatherspoon, C.P., 2000. The use of shaded fuelbreaks in landscape fire management. *For. Ecol. Manage.* 127, 55–66.
- Albini, F.A., 1976. Estimating wildfire behavior and effects. USDA Forest Service, General Technical Report. Intermountain Forest and Range Experiment Station, Ogden, UT, p. 92.
- Anderson, H.E., 1982. Aids to determining fuel models for estimating fire behaviour. USDA Forest Service, General Technical Report INT-122. Intermountain Forest and Range Experiment Station, Ogden, UT, 22 pp.
- Andrews, P.L., 1986. BEHAVE: fire behaviour prediction and fuel modelling system. BURN Subsystem. Part 1. USDA Forest Service, General Technical Report INT-194. Intermountain Forest and Range Experiment Station, Ogden, UT, 130 pp.
- Andrews, P.L., Chase, C.H., 1989. Fire behaviour prediction and fuel modelling system. BURN Subsystem. Part 2. USDA Forest Service, General Technical Report INT-260. Intermountain Forest and Range Experiment Station, Ogden, UT, 93 pp.
- Andrews, P.L., Bevins, C.D., Seli, R.C., 2003. BehavePlus fire modeling system, version 2.0: User's Guide. Gen. Tech. Rep. RMRS-GTR-106WWW. Department of Agriculture, Forest Service, Rocky Mountain Research Station, Ogden, UT, p. 132.
- Bahrenberg, G., Giese, E., Nipper, J., 1992. *Multivariate Statistik. Statistische Methoden in der Geographie Band 2.* Teubner Studienbücher der Geographie. B.G. Teubner, Stuttgart, 415 pp.
- Burgan, R.E., 1987. Concepts and interpreted examples in advanced fuel modelling. USDA Forest Service, General Technical Report INT-238. Intermountain Forest and Range Experiment Station, Ogden, UT, 126 pp.
- Burgan, R.E., Rothermel, R.C., 1984. BEHAVE: fire behaviour prediction and fuel modelling system. FUEL Subsystem. USDA Forest Service, General Technical Report INT-167. Intermountain Forest and Range Experiment Station, Ogden, UT, 126 pp.
- Burrough, P.A., 1981. Fractal dimensions of landscapes and other environmental data. *Nature* 294, 240–242.
- Chandler, C., Cheney, P., Thomas, P., Trabaud, L., Williams, D., 1983. *Forest Fire Behaviour. Fire in Forestry, vol. 1.* John Wiley and Sons, New York, p. 450.
- Chapin, F.S., Matson, P.A., Mooney, H.A., 2002. *Principles of Terrestrial Ecosystem Ecology.* Springer-Verlag, New York, p. 472.
- Chardon, J.P., Adriaensen, F., Matthysen, E., 2003. Incorporating landscape elements into a connectivity measure: a case study for the Speckled wood butterfly (*Pararge aegeria* L.). *Landscape Ecol.* 18, 561–573.
- Coleman, J.R., Sullivan, A.L., 1996. A real-time computer application for the prediction of fire spread across the Australian landscape. *Simulation* 67, 230–240.
- del Barrio, G., Simon, J.C., Cuadrado, A., Sanchez, E., Ruiz, E., Garcia, R., 2000. Aproximacion para estimar la conectividad regional de las redes de conservacion. V Congreso Nacional de Medio Ambiente: Comunicaciones Tecnicas, Madrid, pp. 1–17.
- del Barrio, G., Harrison, P.A., Berry, P.M., Butt, N., Sanjuan, M.E., Pearson, R.G., Dawson, T., 2006. Integrating multiple modelling approaches to predict the potential impacts of climate change on species' distributions in contrasting regions: comparison and implications for policy. *Environ. Sci. Policy* 9, 129–147.
- Duguay, B., Alloza, J.A., Röder, A., Vallejo, R., Pastor, F., 2007. Modeling the effects of landscape fuel treatments on fire growth and behaviour in a Mediterranean landscape (eastern Spain). *Int. J. Wildland Fire* 16, 619–632.
- Duncan, B.W., Schmalzer, P.A., 2004. Anthropogenic influences on potential fire spread in a pyrogenic ecosystem of Florida, USA. *Landscape Ecol.* 19, 153–165.
- Eastman, J.R., 1989. Pushbroom algorithms for calculating distances in raster grids. In: Anderson, E. (Ed.), *Proceedings of*

- the 9th International Symposium on Computer Assisted Cartography, Autocarto 9. Baltimore, MD, pp. 288–297.
- Eastman, J.R., 2001. IDRISI32 release 2. Guide to GIS and Image Processing, vol. 2. Clark Labs, Clark University, Worcester, MA, p. 144.
- Encinas, A.H., Encinas, L.H., White, S.H., del Rey, A.M., Sanchez, G.R., 2007. Simulation of forest fire fronts using cellular automata. *Adv. Eng. Software* 38 (6), 372–378.
- Fernandes, P., Botelho, H., 2004. Analysis of the prescribed burning practice in the pine forest of northwestern Portugal. *J. Environ. Manage.* 70 (1), 15–26.
- Finney, M.A., 1998. FARSITE: fire area simulator-model. Model development and evaluation. USDA Forest Service, Research Paper RMRS-RP-4. Rocky Mountain Research Station, Ogden, UT, 47 pp.
- Finney, M.A., 2001. Design of regular landscape fuel treatment patterns for modifying fire growth and behavior. *Forest Sci.* 47, 219–228.
- Finney, M.A., 2002. Fire growth using minimum travel time methods. *Can. J. For. Res.* 32 (8), 1420–1424.
- Forman, R.T.T., 1995. *Land Mosaics: The Ecology of Landscapes and Regions*. Cambridge University Press, Cambridge, p. 652.
- Frandsen, W.H., 1971. Fire spread through porous fuels from the conservation of energy. *Combust. Flame* 16, 9–16.
- Fujioka, F.M., 2002. A new method for the analysis of fire spread modelling errors. *Int. J. Wildland Fire* 11, 193–203.
- Gardner, R.H., Milne, B.T., Turner, M.G., O'Neill, R.V., 1987. Neutral models for the analysis of broad-scale landscape patterns. *Landscape Ecol.* 1, 19–28.
- Gardner, R.H., Hargrove, W.W., Turner, M.G., Romme, W.H., 1996. Climate change, disturbances, and landscape dynamics. In: Walter, B., Steffen, W. (Eds.), *Global Change and Terrestrial Ecosystems*. International Geosphere-Biosphere Programme Book Series—Book 2. Cambridge University Press, Cambridge, pp. 149–172.
- Gonzalez Rebolgar, J.L., Robles, A.B., De Simon, E., 1999. Las Areas pasto-cortafuegos entre las practicas de gestion y proteccion de los espacios forestales mediterraneos: propuestas de silvicultura preventiva. *Actas de la XXXIX Reunion Cientifica de la Sociedad Espanola para el Estudio de los Pastos*, pp. 146–154.
- Goodwin, B.J., 2003. Is landscape connectivity a dependent or independent variable? *Landscape Ecol.* 18 (7), 687–699.
- Green, D.G., 1983. Shapes of simulated fires in discrete fuels. *Ecol. Model.* 20, 21–32.
- Gustafson, E.J., 1998. Quantifying landscape spatial pattern: what is the state of the art? *Ecosystems* 1, 143–156.
- Gustafson, E.J., Shifley, S.R., Mladenoff, D.J., Nimerfro, K.K., He, H.S., 2000. Spatial simulation of forest succession and harvesting using LANDIS. *Can. J. For. Res.* 30, 32–43.
- Hargis, C.D., Bissonette, J.A., David, J.L., 1998. The behaviour of landscape metrics commonly used in the study of habitat fragmentation. *Landscape Ecol.* 13 (3), 167–186.
- Hargrove, W.W., Gardner, R.H., Turner, M.G., Romme, W.H., Despain, D.G., 2000. Simulating fire patterns in heterogeneous landscapes. *Ecol. Model.* 135, 243–263.
- He, H.S., Mladenoff, D.J., 1999. Spatially explicit and stochastic simulation of forest landscape fire disturbance and succession. *Ecology* 80, 81–99.
- Helfenstein, P., Shepard, M.K., 1999. Submillimeter-scale topography of the lunar regolith. *Icarus* 141, 107–131.
- Hobson, R.D., 1972. Surface roughness in topography: a quantitative approach. In: Chorley, R.J. (Ed.), *Spatial Analysis in Geomorphology*. Methuen & Co., London, pp. 221–245.
- Karafyllidis, I., Thanailakis, A., 1997. A model for predicting forest fire spreading using cellular automata. *Ecol. Model.* 99, 87–97.
- Keane, R.E., Garner, J.L., Schmidt, K.M., Long, D.G., Menakis, J.P., Finney, M.A., 1998. Development of input data layers for the FARSITE fire growth model for the Selway-Bitterroot Wilderness complex, USA. USDA Forest Service General Technical Report RMRS-GTR-3, 66 pp.
- Keane, R.E., Mincemoyer, S.A., Schmidt, K.M., Long, D.G., Garner, J.L., 2000. Mapping vegetation and fuels for fire management on the Gila National Forest Complex, New Mexico, [CD-ROM]. Gen. Tech. Rep. RMRS-GTR-46-CD. U.S. Department of Agriculture, Forest Service, Rocky Mountain Research Station, Ogden, UT, 126 pp.
- Kerby, J.D., Fuhlendorf, S.D., Engle, D.M., 2007. Landscape heterogeneity and fire behavior: scale-dependent feedback between fire and grazing processes. *Landscape Ecol.* 22, 507–516.
- Klinkenberg, B., 1992. Fractals and morphometric measures: is there a relationship? *Geomorphology* 5, 5–20.
- Klinkenberg, B., Goodchild, M.F., 1992. The fractal properties of topography: a comparison of methods. *Earth Surf. Process. Landforms* 17, 217–234.
- Leduc, A., Prairie, Y.T., Bergeron, Y., 1994. Fractal dimension estimates of a fragmented landscape: sources of variability. *Landscape Ecol.* 9, 279–286.
- MAPA-ICONA (Ministerio de Agricultura, Pesca y Alimentación, Dirección General de Conservación de la Naturaleza), 1993. Mapa forestal de España (1:200,000).
- MAPA-ICONA (Ministerio de Agricultura, Pesca y Alimentación, Dirección General de Conservación de la Naturaleza), 1990. Clave fotográfica para la identificación de modelos de combustible.
- Mark, D.M., Aronson, P.B., 1984. Scale-dependent fractal dimensions of topographic surfaces: an empirical investigation, with applications in geomorphology. *Math. Geol.* 16, 671–683.
- Merriam, G., 1984. Connectivity: a fundamental ecological characteristic of landscape patterns. In: Brandt, J., Agger, P. (Eds.), *Proceedings of the 1st International Seminar on Methodology in Landscape Ecological Research and Planning*. Roskilde University, Denmark.
- Michels, E., Cottenie, K., Neys, L., De Gelas, K., Coppin, P., De Meester, L., 2001. Geographical and genetic distances among zooplankton populations in a set of interconnected ponds: a plea for using GIS modelling of the effective geographical distance. *Mol. Ecol.* 10, 1929–1938.
- Miller, C., Urban, D.L., 1999a. A model of surface fire, climate and forest pattern in Sierra Nevada, California. *Ecol. Model.* 114, 113–135.
- Miller, C., Urban, D.L., 1999b. Interactions between forest heterogeneity and surface fire regimes in the southern Sierra Nevada. *Can. J. For. Res.* 29, 202–212.
- Miller, C., Urban, D.L., 2000. Connectivity of forest fuels and surface fire regimes. *Landscape Ecol.* 15, 145–154.
- Miller, J.D., Yool, S.R., 2002. Modelling fire in semi-desert grassland/oak woodland: the spatial implications. *Ecol. Model.* 153, 229–245.
- Mistry, J., Berardi, A., 2005. Assessing fire potential in a Brazilian savanna nature reserve. *Biotropica* 37, 439–451.
- Mladenoff, D.J., He, H.S., 1999. Design and behavior of LANDIS, an object-oriented model of forest landscape disturbance and succession. In: Mladenoff, D.J., Baker, W.L. (Eds.), *Spatial Modeling of Forest Landscape Change: Approaches and Applications*. Cambridge University Press, New York, pp. 125–162.
- Morvan, D., Larini, M., Dupuy, J.L., Fernández, P., Miranda, A.I., Andre, J., Sero-Guillaume, O., Calogine, D., Cuiñas, P., 2004. EUFIRELAB: behaviour modelling of wildland fires: State of the Art. Laboratory for Wildland Fire Sciences and Technologies in the Euro-Mediterranean Region. Deliverable D-03-01, PIF 2004-18, p. 33.
- Outcalt, S.I., Hinkel, K.M., Nelson, F.E., 1994. Fractal physiography? *Geomorphology* 11, 91–106.

- Pausas, J.C., 2003. The effect of landscape pattern on Mediterranean vegetation dynamics: a modelling approach using functional types. *J. Veg. Sci.* 14, 365–374.
- Pardini, G., Gallart, F., 1998. A combination of laser technology and fractals to analyse soil surface roughness. *Eur. J. Soil Sci.* 49, 197–202.
- Peterson, G.D., 2002. Contagious disturbance, ecological memory and the emergence of landscape patterns. *Ecosystems* 5 (4), 329–338.
- Pyne, S.J., 1984. Introduction to wildland fire. In: *Fire Management in the United States*. John Wiley and Sons, New York.
- Riaño, D., Salas, J., Chuvieco, E., 2001. Cartografía de modelos de combustible con teledetección: aportaciones a un desarrollo ambiental sostenible. *Estud. Geogr.* 243, 309–333.
- Riaño, D., Bastarrika, A., Chuvieco, E., Salas, J., Palacios-Orueta, A., 2002. Generation of fuel type maps from Landsat TM images and ancillary data in Mediterranean ecosystems. *Can. J. For. Res.* 32, 1301–1315.
- Röder, A., Kuemmerle, T., Hill, J., Papanastasis, V.P., Tsiourlis, G.M., 2007. Adaptation of a grazing gradient concept to heterogeneous Mediterranean rangelands using cost surface modelling. *Ecol. Model.* 204, 387–398.
- Rothermel, R.C., 1972. A mathematical model for predicting fire spread in wildland fuels. USDA Forest Service, Research Paper INT-115. Intermountain Forest and Range Experiment Station, Ogden, UT, 44 pp.
- Rothley, K., 2005. Finding and filling the “cracks” in resistance surfaces for least-cost modelling. *Ecol. Soc.* 10(1), 4 (online). URL: <http://www.ecologyandsociety.org/vol10/iss1/art4>.
- Russell, W.H., McBride, J.R., 2003. Landscape scale vegetation-type conversion and fire hazard in the San Francisco bay area open spaces. *Landscape Urban Plan.* 64, 201–208.
- Sachs, L., 1982. Applied statistics. In: *A Handbook of Techniques*. Springer-Verlag, New York, p. 706.
- Schneider, K., Robbins, P., 1994. GIS and mountain environments. *Explorations in Geographic Information Systems Technology*, vol. 5. UNITAR (United Nations Institute for Training and Research), Geneva.
- Scott, J.H., Burgan, R.E., 2005. Standard fire behavior fuel models: a comprehensive set for use with Rothermel’s surface fire spread model. USDA Forest Service, General Technical Report RMRS-153. Rocky Mountain Research Station, Fort Collins, CO, 72 pp.
- Shepard, M.K., Campbell, B.A., Bulmer, M.H., Farr, T.G., Gaddis, L.R., Plaut, J.J., 2001. The roughness of natural terrain: a planetary and remote sensing perspective. *J. Geophys. Res.-Planets* 106, 32777–32795.
- Sokal, R.R., Rohlf, F.J., 1995. *Biometry*. In: *The Principles and Practice of Statistics in Biological Research*. W.H. Freeman and Company, New York.
- Stratton, R.D., 2004. Assessing the effectiveness of landscape fuel treatments on fire growth and behavior. *J. For.* 102 (7), 32–40.
- Taylor, P.D., Fahrig, L., Henein, K., Merriam, G., 1993. Connetivity is a vital element of landscape structure. *Oikos* 68, 571–573.
- Tischendorf, L., Fahrig, L., 2000a. On the usage and measurement of landscape connectivity. *Oikos* 90, 7–19.
- Tischendorf, L., Fahrig, L., 2000b. How should we measure landscape connectivity? *Landscape Ecol.* 15, 633–641.
- Theobald, D.M., 2005. A note on creating robust resistance surfaces for computing functional landscape connectivity. *Ecol. Soc.* 10(2), 1 (online). URL: <http://www.ecologyandsociety.org/vol10/iss2/resp1/>.
- Turner, M.G., Gardner, R.H., Dale, V.H., O’Neill, R.V., 1989. Predicting the spread of disturbance across heterogeneous landscapes. *Oikos* 55, 121–129.
- Turner, M.G., Romme, W.H., 1994. Landscape dynamics in crown fire ecosystems. *Landscape Ecol.* 9, 59–77.
- Turner, M.G., Gardner, R.H., O’Neill, R.V., 2001. *Landscape Ecology in Theory and Practice: Pattern and Process*. Springer-Verlag, New York, p. 404.
- Van Wagner, C.E., 1988. Effect of slope on fires spreading downhill. *Can. J. For. Res.* 18, 818–820.
- Velasco, L., 2000. Planificación de redes de áreas cortafuegos. In: Velez, R. (Coordinator), *La Defensa contra Incendios Forestales. Fundamentos y Experiencias*. McGraw-Hill, Madrid, pp. 14.18–14.36.
- Velez, R. (Coordinator), 2000a. *La defensa contra incendios forestales. Fundamentos y experiencias*. McGraw-Hill, Madrid, 1336 pp.
- Velez, R., 2000b. *Selvicultura Preventiva*. In: Velez, R. (Coordinator), *La defensa contra incendios forestales. Fundamentos y experiencias*. McGraw-Hill, Madrid, pp. 14.1–14.18.
- Verbeylen, G., De Bruyn, L., Adriaensen, F., Matthysen, E., 2003. Does matrix resistance influence red squirrel (*Sciurus vulgaris* L. 1758) distribution in an urban landscape? *Landscape Ecol.* 18, 791–805.
- Warntz, W., 1965. A Note on Surfaces and Paths and Applications to Geographical Problems. *The Michigan Inter-University Community of Mathematical Geographers*, pp. 1–22.
- Xu, T., Moore, I.D., Gallant, J.C., 1993. Fractals, fractal dimensions and landscapes. A review. *Geomorphology* 8, 245–262.